UFRRJ

INSTITUTO DE GEOCIÊNCIAS

PROGRAMA DE PÓS-GRADUAÇÃO EM MODELAGEM E EVOLUÇÃO GEOLÓGICA

DISSERTAÇÃO

ESTUDOS PETROLÓGICOS DOS CORPOS SUBVULCÂNICOS DO COMPLEXO ALCALINO DE PASSA QUATRO NA REGIÃO DO PICO DOS TRÊS ESTADOS E ADJACÊNCIAS, NOS ESTADOS DE MG, RJ E SP

GRACIANO CARLOS DE FREITAS

2024

UNIVERSIDADE FEDERAL RURAL DO RIO DE JANEIRO

INSTITUTO DE GEOCIÊNCIAS

PROGRAMA DE PÓS-GRADUAÇÃO EM MODELAGEM E EVOLUÇÃO GEOLÓGICA

ESTUDOS PETROLÓGICOS DOS CORPOS SUBVULCÂNICOS DO COMPLEXO ALCALINO DE PASSA QUATRO NA REGIÃO DO PICO DOS TRÊS ESTADOS E ADJACÊNCIAS, NOS ESTADOS DE MG, RJ E SP

GRACIANO CARLOS DE FREITAS

Sob a Orientação do Professor

Artur Corval

Dissertação submetida como requisito parcial para obtenção dograu de **Mestre em Geociências,** no Curso de Pós-Graduação em Modelagem e Evolução Geológica, Área de Concentração em Geociências.

Seropédica, RJ

Dezembro de 2024

FF862e
e

Freitas, Graciano carlos de , 1982-
Estudos Petrológicos dos Corpos Subvulcânicos do Complexo Alcalino de Passa Quatro na Região do Pico dos Três Estados e Adjacências, nos Estados de MG, RJ e SP. / Graciano carlos de Freitas. - São Miguel do Anta - MG, 2024.
58 f.: il.

Orientador: Artur Corval Vieira.
Dissertação(Mestrado). -- Universidade Federal Rural do Rio de Janeiro, Programa de Pós-Graduação em Modelagem e Evolução Geológica, 2024.

1. Cristalização Fracionada. 2. Fusão Parcial. 3. Rochas Subvulcânicas. 4. Magmatismo Alcalino. I. Vieira, Artur Corval , 1977-, orient. II Universidade Federal Rural do Rio de Janeiro. Programa de Pós Graduação em Modelagem e Evolução Geológica III. Título.

MINISTÉRIO DA EDUCAÇÃO
UNIVERSIDADE FEDERAL RURAL DO RIO DE JANEIRO
INSTITUTO DE GEOCIÊNCIAS

HOMOLOGAÇÃO DE DISSERTAÇÃO DE MESTRADO Nº 89/2024 - IGEO (11.39.00.34)

Nº do Protocolo: 23083.059364/2024-12

Seropédica-RJ, 31 de outubro de 2024.

UNIVERSIDADE FEDERAL RURAL DO RIO DEJANEIRO

INSTITUTO DE GEOCIÊNCIAS

PROGRAMA DE PÓS-GRADUAÇÃO EM MODELAGEM E EVOLUÇÃO GEOLÓGICA

GRACIANO CARLOS DE FREITAS

Dissertação submetida como requisito parcial para obtenção do grau de **Mestre em Geociências,** no Programa de Pós-Graduação em Modelagem e Evolução Geológica, área de concentração em MODELAGEM DE PROCESSOS GEOLÓGICOS E GEODINÂMICOS.

DISSERTAÇÃO APROVADA EM 30/10/2024.

_____

Artur Corval Vieira. Dr. PPGMEG/UFRRJ

(Orientador/Presidente da banca)

_____

Mauro Cesar Geraldes. Dr. UERJ

(Membro Externo)

_____

Renata da Silva Schmitt. Dr. PPGMEG/UFRRJ

(Membro Interno)

(Assinado digitalmente em 01/11/2024 09:43)

ARTUR CORVAL VIEIRA

COORDENADOR CURS/POS-GRADUACAO

PPGMEG (11.39.00.12

Matrícula: ###489#8

(Assinado digitalmente em 04/11/2024 11:05)

RENATA DA SILVA SCHIMITT

ASSINANTE EXTERNO

CPF: ###.###.040-##

(Assinado digitalmente em 31/10/2024 15:03)

MAURO CESAR GERALDES

ASSINANTE EXTERNO

CPF: ###.###.418-##

Visualize o documento original em https://sipac.ufrrj.br/public/documentos/index.jsp informando seu número: **89**, ano: **2024**, tipo: **HOMOLOGAÇÃO DE DISSERTAÇÃO DE MESTRADO**, data de emissão: **31/10/2024** e o código de verificação: **2da375b16b**

AGRADECIMENTOS

A Deus, por me pertmitir usufruir da graça da vida em todos os momentos, os bons e aqueles que de alguma forma podem nos magoar, mas que no fim nos fazem crecer e amadurecer.
Agradeço a meu pai Antônio genuino de Freitas, e minha mãe Maria Helena Rodrigues de Freitas, maiores exemplos de pais que alguem poderia ter. Agradeço meus irmão Claudiano e Vanderlúcio que junto com meus pais, sempre me encorajaram em minhas escolhas.
Agradeço imensamente a minha noiva Cristiane Mara Silva da Costa, pessoa incrível, que esteve ao meu lado 24 horas por dia, minha base nesses tempos.
A Júlio Cesar lopes da Silva, amigo e companheiro de trabalhos de campo com quem aprendi muito nesses anos de convivência.
Agradecimento especial a meu orientador Artur Corval Vieira, pessoa impar com quem tive a honra de conviver durante a graduação e ao longo do desenvolvimento dessa dissertação.
Ao Programa de Pós-graduação em Modelagem e Evolução Geológica (PPGMEG) e a Universidade Federal Rural do Rio de Janeiro (UFRRJ), pela oportunidade. À coordenação do PPGMEG, aos professores e aos meus colegas da turma de 2019, pelo apoio e companheirismo.
Agradeço ao Projeto Petromagmatismo (FAPUR 19/03 e SAP 4600581919 - autorizado pela Agência Nacional de Petróleo, Gás Natural e Biocombustíveis do Brasil) que deu todo apoiou finanseiro a essa pesquisa.

Por fim, agradeço a todos aqueles que, direta ou indiretamente, colaboraram para a realização deste projeto.

O presente trabalho foi realizado com apoio da Coordenação de Aperfeiçoamento de Pessoal de Nivel Superior - Brasil (CAPES) - Código de Financeamento 001. This study was financed in part by the Coordernação de Aperfeiçoamento de Pessoal de Nível Superior - Brasil (CAPES) - Finance Code 001.

RESUMO

FREITAS, Graciano Carlos de. **Estudos petrológicos dos corpos subvulcânicos do Complexo Alcalino de Passa Quatro na região do Pico dos Três Estados e adjacências, nos Estados de MG, RJ e SP**. Dissertação (Mestrado em Modelagem e Evolução Geológica, Geociências). Instituto de Geociências, Departamento de Petrologia e Geotectônica, Universidade Federal Rural do Rio de Janeiro, Seropédica, RJ, 2021.

Esta dissertação apresenta um estudo geológico dos corpos subvulcânicos presentes no Pico dos Três Estados (SP, RJ e MG) e seu entorno no Complexo Alcalino Passa Quatro. Neste estudo, utilizamos dados coletados em campo, dados de petrologia e análises geoquímicas. Os dados petrológicos mostraram que a região estudada apresenta características semelhantes às encontradas na maioria dos corpos alcalinos presentes no litoral sudeste do território brasileiro, principalmente quanto ao teor de feldspato alcalino, tipos de minerais feldspatóides e volume de minerais máficos. A partir de um trabalho de campo mais detalhado, verificamos que a região que parecia apresentar apenas duas litologias em trabalhos anteriores, apresentava um complexo faciológico com pelo menos seis fácies distintas, com destaque para o corpo fonolítico que forma o Pico dos Três Estados (2.665 metros de altura).). Ainda em relação ao trabalho de campo, constatamos que há indícios de processos de mistura de magma na área. A modelagem indica que 10% da cristalização fracionada foi capaz de derivar as rochas fonolíticas de um líquido traquítico baseado nos seguintes elementos: Y, Nb, Yb, Ce, Sm, Eu, La, Nd, Hf e Pr. A fusão parcial modal em lote mostra as possíveis fontes do manto para o magmatismo nesta área. Esses dados apontaram o envolvimento de uma fonte mantélica enriquecida na relação La/Yb em pelo menos 16 vezes mais do que um manto tipo OIB.

Palavras-chave: Cristalização fracionada, fusão parcial, mistura de magma.

ABSTRACT

FREITAS, Graciano Carlos de. **Petrological studies of the subvolcanic bodies of the Passa Quatro Alkaline Complex in the Pico dos Três Estados region and surroundings, in the States of MG, RJ and SP**. Dissertation (Master Science in Geological Modeling and Evolution, Geosciences) Instituto de Geociências, Departamento de Petrologia e Geotectônica, Universidade Federal Rural do Rio de Janeiro, Seropédica, RJ, 2021.

This dissertation presents a geological study of the subvolcanic bodies present in the Pico dos Três Estados (SP, RJ, and MG) and its surroundings at the Passa Quatro Alkaline Complex. In this study, we used field-collected data, petrology and geochemical analysis data. The petrological data showed that the studied region presents similar characteristics to those found in most of the alkaline bodies present in the southeastern coast of Brazilian territory, especially to the contents of alkali feldspar, types of feldspathoid minerals and volume of mafic minerals. From a more detailed fieldwork, we verified that the region that appeared to present only two lithologies in previous works, presented a faciological complex with at least six distinct facies, with emphasis on the phonolitic body that forms the Pico dos Três Estados (2,665 meters high). Still regarded to fieldwork, we found that there are signs of magma mingling processes in the area. Modelling indicates that 10% of fractional crystallization was able to derive the phonolitic rocks from a trachytic liquid based on the following elements: Y, Nb, Yb, Ce, Sm, Eu, La, Nd, Hf and Pr. The modal batch partial melting shows the possible mantle sources for the magmatism in this area. This data pointed out the involvement of an enriched mantle source in the La/Yb ratio by at least 16 times more than an OIB-type mantle.

Keywords: Fractional crystallization, partial melting, magma mingling.

LISTA DE TABELAS

LISTA DE FIGURAS

SUMÁRIO

1 INTRODUÇÃO

1.1 Apresentação

Esta dissertação tem como tema, Estudos Petrológicos dos Corpos Subvulcânicos do Complexo Alcalino de Passa Quatro na Região do Pico dos Três Estados e Adjacências, nos Estados de MG, RJ e SP. Este estudo foi desenvolvido a partir de trabalhos de revisões bibliográficas, trabalhos de campo, estudos em laboratórios envolvendo petrografia e análises geoquímicas. Esta dissertação está estruturada conforme o Manual de Instruções para Organização e Apresentação de Dissertações e Teses na UFRRJ, 3ª edição (2006). A dissertação e a submissão de um artigo científico em periódico de nível B1 ou superior, segundo o Qualis da área de Geociências da CAPES, constituem requisitos para obtenção do título de mestre no Programa de Pósgraduação em Modelagem e Evolução Geológica (PPGMEG) da Universidade Federal Rural do Rio de Janeiro (UFRRJ).

Existem poucos estudos, tratando excluvivamente do aspecto geológico do Complexo Alcalino de Passa Quatro, entre esses estudos destacam-se o de Ulbrich and Gomes, (1981); Brotzu et al. (1992), Chiessi, (2004), Guarino et al. (2019), Silva et al. (2022 e 2024). Todos esses estudos avaliaram o CAPQ em sua totalidade, essa dissertação de mestrado se propôs a estudar os corpos subvulcânicos presentes na porção central deste complexo, apresentamos uma relação de conegeticidade entre esses corpos e caracterizamos uma possível fonte mantélica para os mesmos.

Essa dissertação foi organizada em títulos e subtítulos e os produtos e resultados alcançados estão organizados no formato de artigo científico no título 4. No momento esse artigo se encontra em estágio de avaliação por revista científica especializada.

1.2 Objetivos (Geral e específico)

O objetivo geral deste estudo é compreender a petrogênese associada ao Pico dos Três Estados no Complexo Alcalino de Passa Quatro (PQAC). Além disso, este trabalho tem como objetivos específicos delimitar as áreas de ocorrência de corpos subvulcânicos nesta região e a confecção de um mapa geológico na escala de 1:1.500 do Pico dos Três Estados e entorno.

1.3 justificativa

Esta dissertação contribuirá para aumentar o acervo de estudos geológicos sistemáticos na região (que até o momento é escasso). Isso nos ajudará a trazer respostas para questões petrogenéticas relacionadas aos processos evolutivos e origem do magmatismo félsico alcalino presente nesta região. Os resultados alcançados neste estudo foram baseados em estudos anteriores publicados na literatura científica, trabalhos de campo, dados macro e micro petrográficos, análises litogeoquímicas, envolvendo elementos maiores, traços e terras raras.

1.4 Localização

A área estudada compreende a região que une os Estados de São Paulo, Minas Gerais e Rio de Janeiro, mais precisamente a região conhecida como Pico dos Três Estados (Figura 1). Este pico está a 2.665 metros de altitude com relação ao nível do mar. Está localizado entre as latitudes aproximadas de 22º23" e 22º25" (sul) e longitudes aproximadas de 44º47" e 44º50"

(oeste) no Complexo Alcalino de Passa Quatro (CAPQ), um batólito de formato elíptico com área aproximada de 168 km^2. Tem aproximadamente 70 milhões de anos (Ulbrich e Gomes, 1981; Brotzu et al., 1992; Chiessi, 2004), e está localizado na Província Alcalina da Serra do Mar (Morbidelli et al., 1995; Thompson et al., 1998).

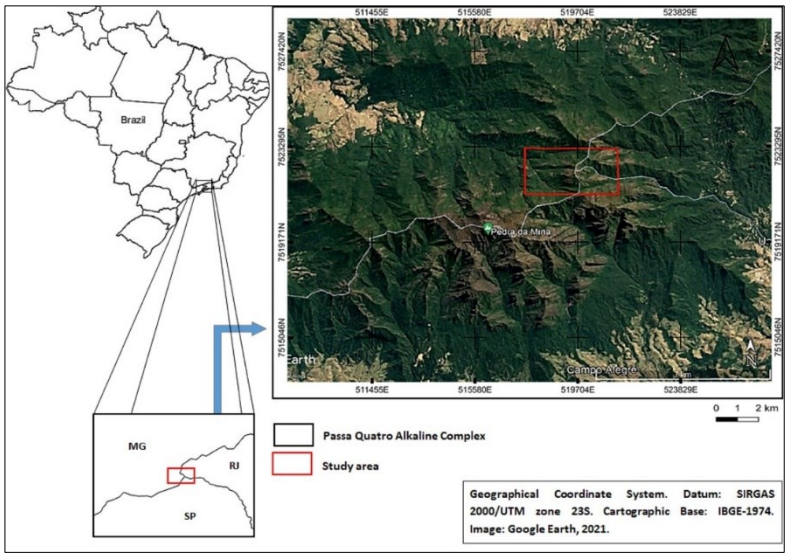

Figura 1. Localização da região estudada compreendendo a área do retângulo vermelho. A figura apresenta uma imagem da área correspondente ao Complexo Alcalino Passa Quatro com destaque para a área de estudo. Fonte: IBGE (1974) e Google Earth, (2021).

2 REVISÃO TEMÁTICA

2.1 Geologia do Complexo Alcalino Passa Quatro

O Complexo Alcalino Passa Quatro (PQAC) constitui uma das vinte e seis intrusões alcalinas que compõem o alinhamento magmático de Cabo Frio proposto por Almeida (1991) como alinhamento de complexos sieníticos com tendência WNW-ESE ao longo de estruturas pré-cambrianas com aproximadamente 60 km de largura e 1.150 km de extensão no sudeste do Brasil. Essa estrutura magmática alinhada juntamente com outras intrusões alcalinas (linha costeira de São Paulo e setor ocidental da Serra da Mantiqueira) denotam a então chamada Província Alcalina Serra do Mar (Ulbrich e Gomes, 1981; Morbidelli et al., 1995; Thompson et al., 1998).

O CAPQ é uma intrusão anelar inserida no sistema de riftes continentais Cenozóicos do sudeste do Brasil (Zalan e Oliveira, 2005; Riccomini et al., 2005; Chiessi, 2004) e corta o domínio Pré-cambriano de Andrelândia (gnaisse, xisto e quartzito) e granitóides colisionais do Orógeno Ribeira no setor central da Província Mantiqueira (Heilbron et al., 2020). Os afloramentos de contato do embasamento com o CAPQ são escassos e difíceis de encontrar devido à grande quantidade de depósitos de tálus e à extensa cobertura vegetal/florestal (Sigolo, 1988; Chiessi, 2004).

De acordo com os trabalhos anteriores relacionados ao CAPQ (Brotzu et al., 1992; Sigolo et al., 1992; Chiessi, 2004; Guarino et al., 2019), o complexo é formado por três intrusões de anéis concêntricos compostos por rochas alcalinas, subsaturadas em sílica, leucocráticas, predominantemente maciças, de granulação grossa a média, caracterizadas como: nefelina sienitos maciços, distribuídos de forma predominante ao longo do complexo; nefelina microsienitos, traquitos localizados na porção central e brechas magmáticas alcalinas com ocorrência na porção central e noroeste do CAPQ; (Figura 2).

O magmatismo máfico do CAPQ se apresenta na forma de diques espessuras centimétricas a métricas- que cortam as rochas do embasamento próximas ao contato com o complexo e possivelmente constituem o magma parental das rochas félsicas presentes no CAPQ, (Thompson et al., 1998; Marins, 2012; Silva et al., 2022). Adicionalmente, Chiessi (2004) descreve diques de lamprófiros alcalinos com espessuras que variam de 2 a 4 decímetros que cortam rochas plutônicas na porção centro-sul do CAPQ. A idade K-Ar para anfibólio de nefelina sienito do PQAC é 66,7 ± 3,3 Ma (Sonoki e Garda, 1988). As idades Rb-Sr de rocha total para nefelina sienitos consistem em 77 ±3 (Brotzu et al., 1992) e 70,4 ±0,5 Ma (Montes-Lauar et al., 1995).

2.2 Geologia da área de estudo

As rochas predominantes na região de estudo são classificadas como nefelina sienito, álcali sienitos com nefelina e álcali sienitos, cortadas por diques de fonolito e traquito, além de um corpo fonolítico localizado na região central e mais alta da área, conhecida como Pico dos Três Estados, (Figura 7B). A área onde está localizado este corpo fonolítico foi classificada em trabalho anterior (Chiessi, 2004) como traquito (Figura 2), porém, propomos uma reclassificação desta rocha subvulcânica com base em estudos mais detalhados a nível de trabalho de campo, petrografia microscópica e análises geoquímicas.

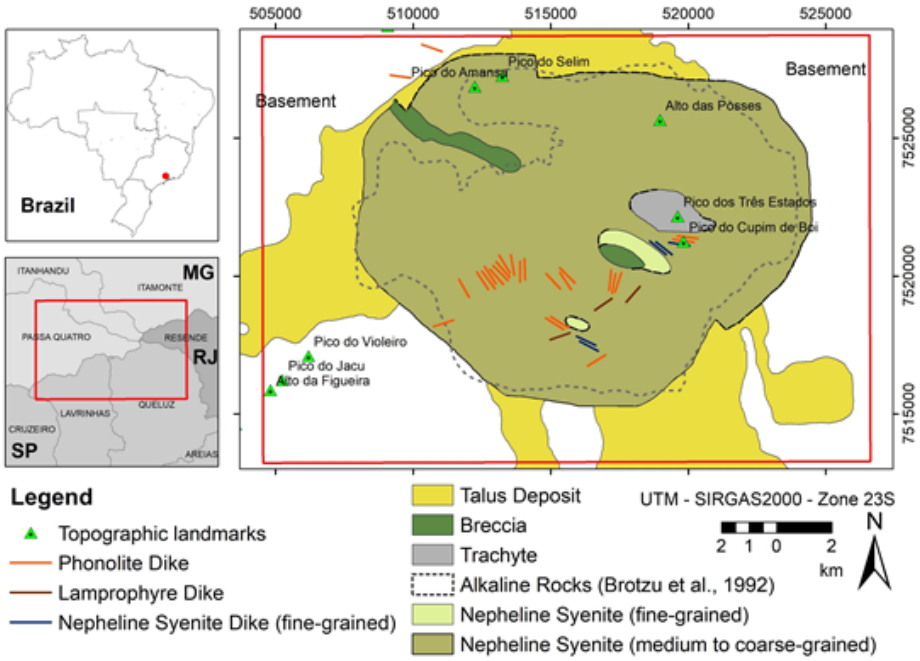

Figura 2. Mapa geológico simplificado do Complexo Alcalino de Passa Quatro, adaptado de Brotzu et al. (1992) e Chiessi (2004).

Chiesse (2004) descreve a pouca diferença existente entre traquitos e fonolitos na área de estudos com base na composição mineralógica dessas litologias, basicamente a diferença consiste na ausência ou menor quantidade de nefelina, algo inferior a 5% em volume e no volume de piroxênio que também é inferior a 5% nos traquitos. A figura 3 apresenta um contato entre essas duas litologias identificado pela linha tracejada de cor preta, a olho nu essas duas litologias são muito semelhantes, tanto na coloração que é acinzentada, quanto na textura que é de forma geral maciça. De acordo com Wilson (1989), os fonolitos podem ser líquidos residuais de séries de diferenciação subsaturadas em sílica e alcalinas intermediárias. Essa relação, em certa medida nos dá direcionamento ao longo dos trabalhos a uma proposição de cogeneticidade entre essas duas litologias.

Os distintos tipos de intrusões (dique em anel, dique tabular e plugs), além de brechas subvulcânicas, evidenciam estágio crustal raso de instalação de fonolitos e traquitos no PQAC (Silva et al., 2022). No entanto, não há informações sobre a relação espacial (por exemplo, possível justaposição) e temporal (por exemplo, coexistência) dessas litologias subvulcânicas distintas (fonolitos e traquitos) na região de estudo. Além disso, não há uma descrição petrográfica detalhada dos subtipos de fonolitos e traquitos (faciologia) para esta região do PQAC. Somando-se a isso, a falta de dados litogeoquímicos da região não possibilita um aprofundamento envolvendo estudos petrológicos, tanto no que diz respeito à diferenciação magmática (cogeneticidade) quanto às características da fonte geradora do plug fonolítico que compõe o Pico dos Três Estados.

Para resolver esses problemas petrológicos, integramos dados de geologia de campo, petrografia e litogeoquímica (principais óxidos e elementos traços) com modelagem de processos magmáticos (por oligoelementos) para avaliar a possível cogeneticidade entre os traquito e fonólitos caracterizados na região e a provável fonte geradora desse magmatismo alcalino.

Figura 3. A imagem apresenta a semelhança entre o traquito (T) e o fonolito (F), com relação a coloração e a textura. A linha tracejada marca o contato entre essas litologias, e o cabo da marreta aponta para o norte. Fonte: arquivo pessoal Fonte: arquivo pessoal.

3 MATERIAIS E MÉTODOS

Neste capítulo serão apresentados os materiais, métodos e técnicas utilizados para atingir os objetivos propostos para esta dissertação. O processo de construção desse trabalho foi dividido em quatro etapas, sendo elas: a revisão de literatura, trabalhos de campo, petrografia e litogeoquímica. Cada uma dessas etapas será descrita a seguir.

3.1 Revisão de Literatura

A revisão de literatura foi a primeira etapa desse trabalho. Apesar de não haver uma extensa bibliografia tratando do aspecto geológico do Complexo Alcalino de Passa Quatro foi possível montar um bom planejamento das atividades de campo com as referências utilizadas (Thompson et al., 1998; Marins, 2012; Chiessi, 2004; Sonoki e Garda, 1988; Brotzu et al., 1992; Montes-Lauar et al., 1995). Em particular, foi o trabalho de Chiessi, 2004 que despertou a atenção para os corpos Subvulcânicos presentes no Pico dos Três Estados, constituindo assim a principal motivação para a realização desse trabalho.

3.2 Trabalho de campo

A região de estudo, que abrange cerca de 25 km^2, está localizada em altitudes próximas e a 2.665 metros de altitude, cota mais elevada da área que é o marco de interseção entre os Estados De SP, MG e RJ, compreendo uma das regiões mais elevadas do Sudeste brasileiro e de acesso exclusivamente por trilhas, tornando-a uma área de difícil exploração. Para alcançar a área de estudos é necessária uma caminhada de aproximadamente quinze horas, com carga individual de equipamentos e suprimentos variando de vinte a trinta quilos. A quantidade de suprimentos foi calculada para os oito integrantes do grupo para um total de seis dias de acampamento. Para o mapeamento geológico da área, utilizamos como base as folhas topográficas de Passa Quatro na escala 1:50.000, segundo IBGE (1974).

Setenta estações descritivas foram georreferenciadas e descritas. A ocorrência de afloramentos e blocos, bem como quaisquer alterações na mineralogia, modo, textura e estrutura (magmática e não-magmática) dessas rochas foram anotadas e fotografadas em campo.

3.3 Petrografia

Dezoito das vinte e nove amostras de rochas coletadas na etapa de campo foram utilizadas para a confecção de vinte e oito seções polidas, as amostras não apresentavam processos de alteração e foram selecionadas visando uma maior representatividade de rochas características da região de estudo (Best, 2002). A SOLINTEC (Serviços Integrados de Geologia) foi a empresa responsável pela confecção dos perfis polidos. As análises microscópicas de luz transmitida foram realizadas em instrumental ZEISS AXIO (Figura 4), conectado a um computador para aquisição de fotomicrografias no Laboratório de Modelagem e Evolução Geológica (LabMEG) da Universidade Federal Rural do Rio de Janeiro (UFRRJ).

Figura 4. Microscópio ZEISS AXIO utilizado para estudo microscópico de lâminas petrográficas. Fonte: Arquivo pessoal.

O estudo da granulometria (fina <1mm, média 1-3mm e grossa >3mm), classificação textural e hábitos minerais dos grãos, entre outras características mineralógicas foram baseadas em Gill (2014), Mackenzie et al. (1982) e Hibbard (1995). As classificações litológicas foram baseadas no estudo de Le Maitre (2002).

3.4 Litogeoquímica

As dezoito amostras previamente descritas ao microscópio foram inicialmente preparadas para análise litogeoquímica nas instalações do LabMEG e do Departamento de Petrologia e Geotectônica da UFRRJ. Esta preparação inicial visou a fragmentação manual das amostras de rocha até o tamanho de 10mm^2, seguida do descarte dos fragmentos não representativos, lavagem com água destilada dos fragmentos, secagem e armazenamento em embalagem.

Posteriormente, os fragmentos foram pulverizados em malha menor que 200 mesh durante trinta segundos em um moinho de panelas (Figura 5) do tipo sheatbox de carbeto de tungstênio da marca Comercial Siebtechnik, procedimento realizado no Laboratório de Preparação de Amostras da Universidade Federal do Rio de Janeiro (UFRJ), segundo critérios estabelecidos por Best (2002). Aproximadamente dez gramas de pó foram colocados em frascos apropriados e enviados para Activation Laboratories Ltd (ACTLABS) no Canadá, onde os principais óxidos e oligoelementos, incluindo elementos de terras raras (REE), foram analisados por ICP-OES e ICP-MS. Mais detalhes sobre instrumentais, rotinas e material certificado podem ser encontrados em actlabs.com.

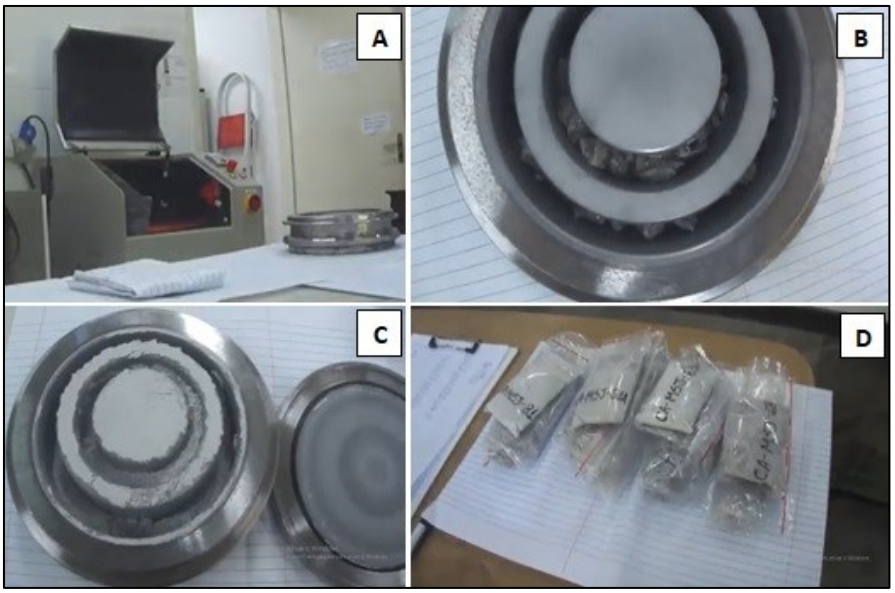

Figura 5. Equipamento utilizado para moagem das amostras; (A) moinho de panela; (B) panela de tungstênio com fragmentos de rocha antes da moagem; (C) panela de tungstênio com o pó resultante da moagem; (D) embalagens com o pó obtido no processo, etiquetadas conforme a identificação das amostras. Fonte: Arquivo pessoal

3.4.1 Procedimentos analíticos litogeoquímicos

O laboratório ACTLABS no Canadá analisou as amostras usando o pacote 4litho que envolve a análise predominantemente de óxidos maiores por ICP-OES após a fusão da amostra com metaborato ou tetraborato de lítio. Os oligoelementos são analisados por ICP-MS e a perda de ignição (LOI) foi quantificada por gravimetria. Os óxidos maiores são representados em porcentagem (% em peso), enquanto os oligoelementos são representados em partes por milhão (ppm) e todo o ferro presente nas amostras foi analisado como ferro total na forma de ferro férrico ($Fe_2O_3^t$). A detecção de óxidos maiores é inferior a 0,01%, enquanto os oligoelementos variam entre 20 a 0,002 ppm, e o limite de detecção de REE alcança 0,05 ppm.

Qualquer método analítico envolve precisão e exatidão sendo que a precisão é a capacidade de repetir resultados, enquanto a exatidão é o mais próximo que você pode chegar do valor correto. O pacote 4litho utiliza dados de doze padrões internacionais de rochas para avaliar a precisão dos dados obtidos. O padrão SY-4 (sienito) foi utilizado como referência devido à semelhança com as rochas da área de estudo.

As precisões analíticas para os elementos principais variam de 0 a 1,9%. A precisão analítica para elementos menores varia de 0 a 13,3%. Para os oligoelementos, a precisão analítica varia de 0 a 15,9%. Apenas Cr não apresentou valores detectáveis. A precisão analítica para os elementos principais varia de 0,1 a 7,4%. A precisão analítica para elementos menores varia entre 7,1 e 12,5%. Para oligoelementos, a precisão analítica varia de 0 a 6,2%.

Os dados geoquímicos obtidos incluem: 1) óxidos principais (SiO_2, TiO_2, Al_2O_3, $Fe_2O_3^t$, MnO, MgO, CaO, Na_2O, K_2O, P_2O_5 e LOI, 2) oligoelementos móveis incompatíveis (Ba, Rb e Sr), imobilizar incompatíveis (Zr, Y e Nb,), compatíveis (Ni, Cr, V, Co,), elementos de terras raras (La, Ce, Pr, Nd, Sm, Eu, Gd, Tb, Dy, Ho, Er, Tm, Yb e Lu,) e U, Th, Hf e Pb.

A interpretação geoquímica baseou-se, fundamentalmente, no software GeoChemical Data ToolKIT (GCDkit; Janoušek et al., 2006), adequado para discriminação de séries,

classificação de rochas, cálculo CIPW (Tabela 3) e interpretação petrogenética. Os valores de LOI das amostras selecionadas para este estudo estão, em geral, abaixo de 2% (média 1,73%; Tabela 1).

Rochas com altos valores de LOI são geralmente mais alteradas do que aquelas com valores mais baixos (Valente et al., 2002). Algumas amostras deste trabalho apresentaram valores de LOI acima de 2%. Contudo, deve-se notar que além dos efeitos de alteração da rocha, as determinações de LOI são suscetíveis a erros de medição significativos, por exemplo, ganho de peso devido à oxidação do ferro ferroso (Lechler & Desilets, 1987). Uma estimativa da qualidade das análises aqui utilizada foi o cálculo dos coeficientes de variação (coeficiente de variação = desvio padrão/média; Tabela 1).

4 ARTIGO CIENTÍFICO: SUBVOLCANIC PETROLOGY OF THE PICO DOS TRÊS ESTADOS REGION (SE BRAZIL): IMPLICATIONS FOR ALKALINE MAGMATIC EVOLUTION

Graciano Carlos Freitas[1*], Artur Corval[1], Júlio Cesar Lopes da Silva[2], Sérgio de Castro Valente[1], Helena Saraiva Koenow Pinheiro[1]

[1]Postgraduate Program in Modeling and Geological Evolution of the Federal Rural University of Rio de Janeiro, Agronomy Institute/Department of Petrology and Geotectonics. Rodovia BR 465, km 7 - CEP: 23.890-000 - Seropédica - RJ - Brazil

[2]Postgraduate Program in Geology of the Federal University of Rio de Janeiro, Institute of Geosciences, Athos da Silveira Ramos, 274, block G. Cidade Universitária, Ilha do Fundão. CEP 21.941-916 Rio de Janeiro - RJ - Brazil.

* Corresponding author.

E-mail address: gracianoufrrj@hotmail.com

4.1 Abstract:

This paper presents a geological study of the subvolcanic bodies present in the Pico dos Três Estados (São Paulo (SP), Rio de Janeiro (RJ), and Minas Gerais (MG)) and its surroundings at the Passa Quatro Alkaline Complex. In this study, we used field-collected data, petrography, and geochemical analysis data. From a more detailed fieldwork, we verified that the region that appeared to present only two lithologies in previous works presented a faciological complex with at least six distinct facies, with emphasis on the phonolitic body that forms the Pico dos Três Estados (2,665 m high). Still regarding fieldwork, we found that there are signs of magma mingling processes in the area. Modeling indicates that 10% of fractional crystallization was able to derive the phonolitic rocks from a trachytic liquid based on the following elements: Y, Nb, Yb, Ce, Sm, Eu, La, Nd, Hf, and Pr. The modal batch partial melting shows the possible mantle sources for the magmatism in this area. This data pointed out the involvement of an enriched mantle source in the La/Yb ratio by at least 16 times more than an Oceanic Island Basalt (OIB)-type mantle.

KEYWORDS: fractional crystallization; partial melting; magma mingling; subvolcanic rocks.

4.2 Introduction

The studied area comprises the region that joins the States of São Paulo, Minas Gerais, and Rio de Janeiro, more precisely known as Pico dos Três Estados (Fig. 6). This peak is 2,665 m high and is located between the approximate latitudes of 22º20' and 22º30' (south) and the approximate longitudes of 44º45' and 45º00' (west) in the Passa Quatro Alkaline Complex (PQAC), which is an elliptical-shaped batholith with an approximate area of 165 km^2 (Chiessi, 2004). It is 70 million years old (Brotzu et al., 1992; Ulbrich & Gomes, 1981), and is located in the Serra do Mar Alkaline Province (Morbidelli et al., 1995; Thompson et al., 1998).

This paper will contribute to increasing the collection of systematic geological studies in the region (which has been scarce until now). It will help us to bring answers to petrogenetic questions related to the evolutionary processes and source of the felsic magmatism in this region.

The main objective of this study was to understand the petrogenesis associated with the subvolcanic bodies present in Pico dos Três Estados in the Passa Quatro Alkaline Complex and in the region around the peak.

Furthermore, this work proposed to delimit the occurrence areas of these subvolcanic bodies, which allowed the creation of a geological map on a scale of 1:1,500 of the entire area involved in the study. The results achieved in this article were based on previous studies published in scientific literature, fieldwork, macroscopic and microscopic petrographic data, and lithogeochemical analyses (main oxides, traces, and rare earth elements).

We applied all these data to the construction of geochemical models to define the evolutionary processes involved in the petrogenesis of magmatism in the studied region.

4.3 Geological setting

4.3.1 Geology of the Passa Quatro Alkaline Complex

The PQAC constitutes one of the 26 alkaline intrusions that comprise the Cabo Frio magmatic alignment proposed by Almeida (1991) as an alignment of syenitic complexes WNW-ESE trending along Precambrian structures with approximately 60 km of wide and 1,150 km of extension in the southeast of Brazil. This aligned magmatic structure together with other alkaline intrusions (São Paulo coastal line and occidental sector of Mantiqueira Mountain Range) denotes, so previously called, Serra do Mar Alkaline Province (Morbidelli et al., 1005; Thompson et al., 1998; Ulbrich & Gomes, 1981).

The PQAC is a ring intrusion inserted in the Cenozoic continental rift system of southeast Brazil (Chiessi, 2004; Riccomini et al., 2005; Zalán & Oliveira, 2005) and crosscut the Precambrian Andrelândia domain (gneiss, schist, and quartzite) and collisional granitoids from the Ribeira orogen in the central sector of the Mantiqueira Province (Heilbron et al., 2020). The contacts between the basement and the PQAC are difficult to delimit due to the large amount of talus deposits and the extensive forest cover present on the complex edges (Chiessi, 2004; Sigolo, 1988).

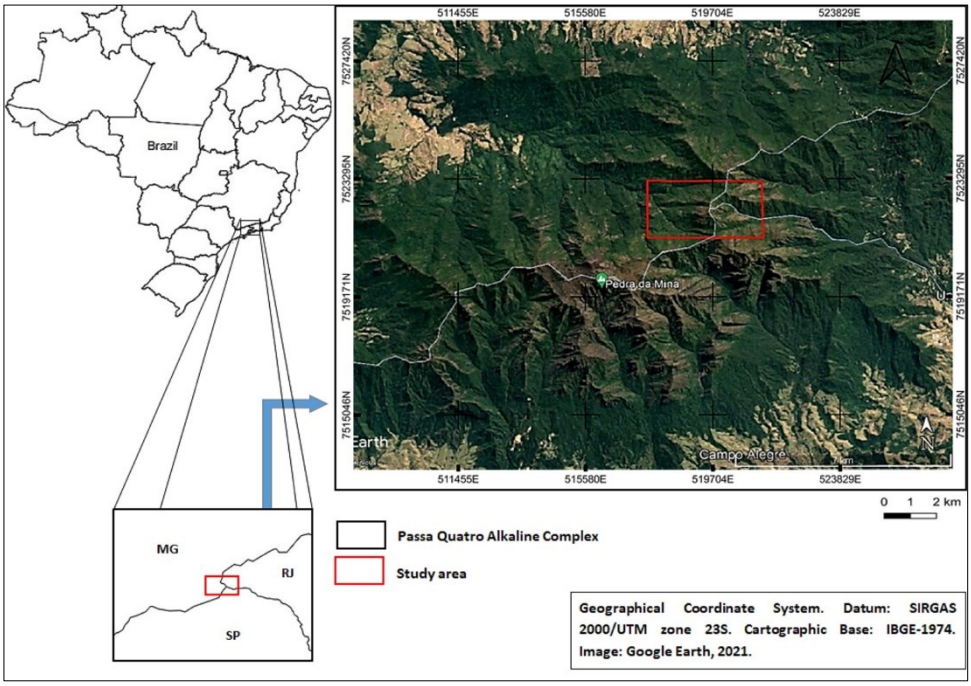

Figure 6. Location of the studied region within the red rectangle. The figure shows the area corresponding to the Passa Quatro Alkaline Complex, highlighting the specific study area. Source: IBGE (1974) and Google Earth, (2021).

Previous work (Brotzu et al., 1992; Chiessi, 2004; Guarino et al., 2019; Sigolo et al., 1992) has suggested that the PQAC is predominantly formed by moderately and strongly silica-undersaturated syenites (Fig. 7A).

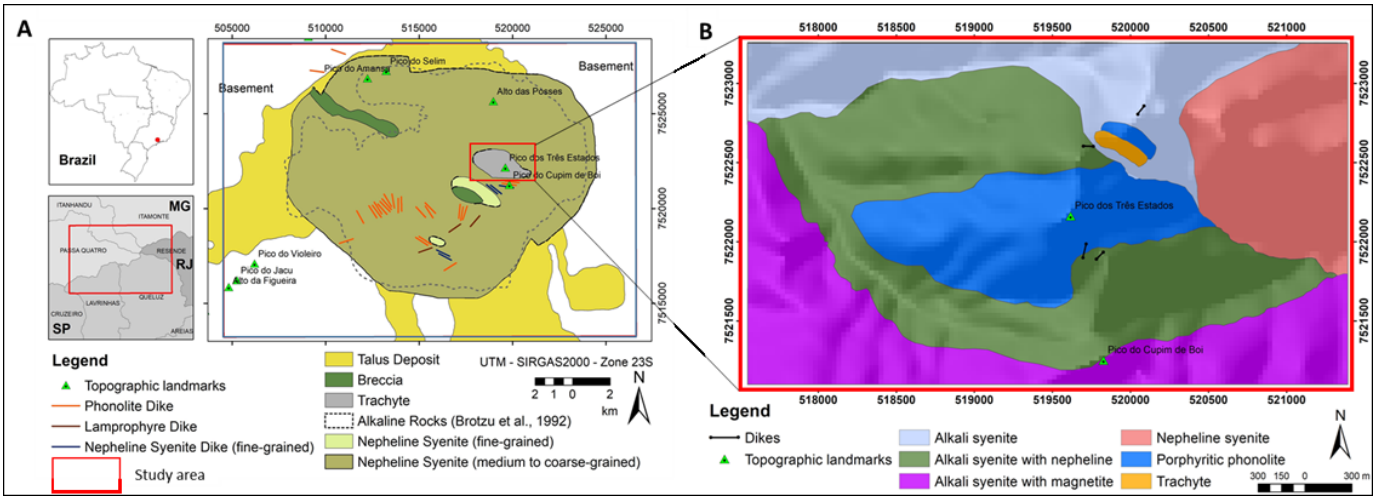

Figure 7. **A**: Simplified geological map of the Passa Quatro Alkaline Complex. Modified from Brotzu et al. (1992) and Chiessi (2004). **B**: Simplified geological map of the studied area showing only the outcropping lithologies represented on the map. UTM coordinate System. Datum: SIRGAS 2000/UTM zone 23S.

Centimeter-to-metric thickness dikes represent the mafic magmatism of the PQAC, which cut the basement rocks close to the contact with the complex and are possibly representatives of the felsic subvolcanic rocks' parental magma characterized in the complex (Marins, 2012; Silva., 2024; Thompson et al., 1998). Additionally, Chiessi (2004) has described the occurrence of lamprophyre's dikes with thicknesses ranging from 2 to 4 cm, which cut plutonic rocks located in the innermost portions of the PQCA. The K-Ar age for amphibole isolated in nepheline syenite is 66.7 ± 3.3 Ma (Sonoki & Garda, 1988). The Rb-Sr ages for whole-rock nepheline syenites are 77 ± 3 (Brotzu et al., 1992) and 70.4 ± 0.5 Ma (Montes-Lauar et al., 1995).

4.3.2 Geology of the study area

There are few geological studies published in the literature dedicated to the Pico dos Três Estados subvolcanic plug. Chiessi's work (2004) refers to the plug as a trachytic body with an area of approximately 8.25 km², which corresponds to 5% of the total area of the PQAC. For the same author, the plug is characterized as a sigmoidal geometry with a main orientation in WNWESE, very fine grain, and aphyric to porphyritic textures.

The study region's predominant plutonic rocks are classified as alkali syenite with nepheline and alkali syenites, cut by phonolite, lamprophyre, and trachyte dikes. In the central and highest region of the area, known as Pico dos Três Estados, we identified a phonolite (Fig. 7B). The area where this plug is located was classified in previous work (Chiessi, 2004) as trachyte (Fig. 7A; however, we propose a reclassification of this subvolcanic rock based on more detailed studies.

The different types of intrusions (ring dike, tabular dike, and plug), in addition to subvolcanic breccias, show a shallow crustal stage of installation of phonolites and trachytes in the PQAC with evidence of volcanism (Silva et al., 2022). However, there is no information on the spatial (e.g., possible juxtaposition) and temporal (e.g., coexistence) relationship of these distinct subvolcanic lithologies (phonolites and trachytes) in the study region. Furthermore, there are no phonolite and trachyte subtypes with detailed petrographic descriptions in previous works for this region of the PQAC. Adding to this, the lack of lithogeochemical data in the region configures the absence of the petrological hypothesis magmatic differentiation (cogeneticity) and the characteristics of the source generating the phonolite plug that makes up Pico dos Três Estados.

To solve these petrological problems, we integrated data from field geology, petrography, and lithogeochemistry (main oxides and trace elements) with modeling of magmatic processes (by trace elements) to evaluate the supposed trachyte-phonolite cogeneticity and the generating source of the alkaline magmatism present in the focus area of this study.

4.4 Materials and methods

The materials for this work are rocks collected from outcrops in Pico dos Três Estados and its surroundings during the field geology stages in the eastern region of the PQAC. Posteriorly, aliquots of these materials were disponible to polished section confection (for microscopic petrography) and whole-rock powder (for lithogeochemistry).

4.4.1 Fieldwork

The study region comprises one of the highest elevations in the Brazilian Southeast, and access is exclusively by trails, making it difficult to access. We need to walk approximately 15 h to reach the study area, which is approximately 25 km^2. For the geological mapping, we used the topographic sheet of Passa Quatro as a cartographic basis at a scale of 1:50,000, according to IBGE (1974).

Seventy description stations were systematically georeferenced and described. The occurrence of outcrops and pebbles was noted and photographed in the field, together with changes in the mineralogy, mode, texture, and structure (magmatic and nonmagmatic) of these rocks.

4.4.2 Petrography

We have made 28 polished sections from 18 samples collected. SOLINTEC (Integrated Geology Services) was the company responsible for making the polished profiles. Transmitted light microscopic analyses were carried out using a ZEISS AXIO instrument, connected to a computer to acquire photomicrographs, at the Geological Modeling and Evolution Laboratory (LabMEG) of the Universidade Federal Rural do Rio de Janeiro (UFRRJ).

We based the granulometry (fine < 1 mm, medium 1–3 mm, and coarse > 3 mm), textural classification, and mineral grain habits, among other mineralogical characteristics, on Gill (2014), Hibbard (1995), and Mackenzie et al. (1982). The lithological classifications were according to Le Maitre et al. (2002).

4.4.3 Lithogeochemistry

Part of the samples previously described under the microscope were initially prepared for lithogeochemical analysis at the facilities of LabMEG and the Department of Petrology and Geotectonics at UFRRJ. This initial preparation consists of manually fragmenting rock samples to a size of 10 mm^2, followed by discarding non-representative fragments, washing the fragments with distilled water, drying, and storing.

Subsequently, the fragments underwent a grinding process in a Siebtechnik tungsten pan mill. For this stage, we used the Sample Preparation Laboratory at the Universidade Federal do Rio de Janeiro (UFRJ) and followed the criteria established by Best (2002). Approximately 10 g of powder was placed in appropriate vials and sent to Activation Laboratories Ltd. (ACTLABS) in Canada, where the main oxides and trace elements, including rare earth elements (REE), were analyzed by inductively coupled plasma optical emission spectroscopy (ICP-OES) and inductively conductively plasma mass spectrometry (ICP-MS).

4.4.3.1 Lithogeochemistry analytical procedures

The ACTLABS laboratory in Canada analyzed the samples using the 4litho package. The 4litho package involves the analysis of larger oxides by ICP-OES after fusing the sample with metaborate or lithium tetraborate. ICP-MS analyzes trace elements, and loss of ignition (LOI) was quantified by gravimetry. The main oxides are represented in percentage (% by weight). In contrast, trace elements are defined in parts per million (ppm), and all iron present in the samples was analyzed as total iron in the form of ferric iron ($Fe_2O_3^t$).

The detection limit for major oxides is less than 0.01%, while trace elements range from

20 to 0.002 ppm, and for REE it goes up to 0.05 ppm (Table 1). Any analytical method involves precision and accuracy. Precision is the ability to repeat results, while accuracy is the closest you can get to the correct value. The 4litho package uses data from twelve international rock standards to evaluate the accuracy of the data obtained. We have adopted SY-4 syenite as the standard due to its similarity with the study area rocks.

Precision for major elements ranges from 0 to 1.9%, for minor elements it ranges from 0 to 13.3%, and for trace elements from 0 to 15.9%. Only Cr did not present detectable values. The accuracy for major elements ranges from 0.1 to 7.4%; for minor elements, it ranges between 7.1 and 12.5%; and for trace elements, the range is 0 to 6.2%.

The geochemical data obtained include main oxides (SiO_2, TiO_2, Al_2O_3, $Fe_2O_3^t$, MnO, MgO, CaO, Na_2O, K_2O, P_2O_5, and LOI), mobile incompatible trace elements (Ba, Rb, and Sr), immobile incompatibles (Zr, Y, and Nb), compatible (Ni, Cr, V, and Co), rare earth elements (La, Ce, Pr, Nd, Sm, Eu, Gd, Tb, Dy, Ho, Er, Tm, Yb, and Lu), and U, Th, Hf, and Pb (Table 2).

The geochemical interpretation was based, fundamentally, on the software GeoChemical Data ToolKIT (GCDkit; Janousek et al., 2006), suitable for series discrimination, rock classification, CIPW (Table 3) calculation, and petrogenetic interpretation.

The LOI values of the samples selected for this study are, in general, below 2% (mean 1.73%; Table 1). High LOI values in rocks are generally more altered than those with lower values (Valente et al., 2002). Some samples of this work had LOI values above 2%. However, it should be noted that in addition to the rock alteration effects, LOI determinations are susceptible to significant measurement errors, for example, weight gain due to ferrous iron oxidation (Lechler & Desilets, 1987).

A quality estimate of the analyses used here was the calculation of coefficients of variation (coefficient of variation = standard deviation/mean; Table 1). According to Cox et al. (1979), Rollinson (1993), and Rollinson and Pease (2021), high values of coefficients of variation are indicative of:

1. Analytical error that can be tested with precision and accuracy data;
2. Weathering that this can be tested by checking the LOI values and variations of immobile incompatible trace elements, e.g., Y, Zr, and Nb.

Only P_2O_5, Ba, and Sr elements analyzed in the studied samples had a variation coefficient above 1. Possibly, this was due to the fact of some weathering according to item 2 above, since the precision and accuracy values were considered satisfactory.

Analytical results of lithogeochemical data from elements of 18 samples are shown in Table 1.

4.4.4 Geochemical modeling

It was intended that the petrogenesis of the magmatism associated with the study area would be based on regression analysis by the least squares method. Thus, variation diagrams would be elaborated for major elements, mobile incompatible, and immobile incompatible trace elements. In this way, it would be possible to discuss the evolutionary processes that would have occurred in the magmatic chambers during the generation of the trachytic and phonolitic bodies of the PQAC.

We have chosen to work with the modal batch partial melting model with trace elements to characterize the generating source of magmas from Três Estados plug in the PQAC. We used

the Fractional Crystallization Model with trace elements to test the hypothesis of cogeneticity between the trachytes and phonolites of the Três Estados plug, for which we used the Rayleigh equation.

4.5 Results

4.5.1 Fieldwork

We organized the field activities in two stages: firstly, we prioritized a geological profile on the north side of the study area, including the highest region where the intersection boundaries of the Three States are located. Second, we prioritized the south face in a profile that connects the top of Pico dos Três Estados to the base of the neighboring peak known as Cupim do Boi.

We collected 29 samples, divided into 16 subvolcanic and 13 plutonic rocks. In the subvolcanic rocks, the predominant texture is porphyritic, and the predominant color is dark to medium gray (Fig. 8A-B). The plutonic rocks are inequigranular to equigranular, with a light gray color due to the low volume of mafic minerals, not exceeding 10% of the rock's volume.

In some points of the alkali syenite, one of the plutonic rocks characterized in the field, we identified semicircular portions (Fig. 8C), with a major axis varying between 1 and 6 cm. This material is rich in mafic minerals in a proportion that varies from 35 to 45% of the modal composition, different from the host rock, which had a maximum of 10% of mafic minerals in its composition. According to Furman and Spera (1985) and Lai et al. (2008), characteristics such as the facoidal or rounded shape of enclaves and the mineralogical difference between the host rock and the enclaves suggest the occurrence of magma mingling.

The prominent feature in the area is the porphyritic phonolite plug, which represents a rock formation measuring approximately 1.2 km^2, including the highest peak in the study area. The predominant lithology in contact with the phonolite plug is alkali syenite with nepheline (Fig. 8D), however, in the northeast portion of the plug, we identified contacts with two other lithologies: alkali syenite and nepheline syenite (Figs. 7B and 8E-F).

Figure 8 shows macroscopic images of the lithologies characterized in the field and confirmed with photomicrographs and geochemical analysis.

4.5.2 Petrography

The microscopic description of the 28 thin sections from samples collected revealed the existence of six distinct lithologies.

Four of these rocks (alkali syenite, alkali syenite with nepheline, trachyte, and porphyritic phonolite) were mapped as units, and the other two (nepheline syenite with sodalite and mesocratic monzosyenite) occur only as inclusions present in the mapped units. These lithologies will be described in the following section, and the photomicrographs are shown in figure 9.

Lithology 1: Alkali syenite.

This lithology (Fig. 9A) is holocrystalline isotropic with coarse to fine granulometry (5 to > 0.5 mm), composed essentially of alkali feldspar crystals. These alkali feldspar crystals have imbrication texture and represent 91% of the volume sample, and interstitial of them occur

nepheline (4% vol.), brown hornblende (3% vol.), Fe-Ti oxide (1% vol.), sphene (1% vol.), and minor biotite, aegirine-augite, apatite, and zircon crystals.

Lithology 2: Nepheline syenite with sodalite.

The nepheline syenite (Fig. 9B) with sodalite is holocrystalline, inequigranular, composed of approximately 76% alkali feldspar, 10% nepheline, 4% sodalite, 1% biotite, and 1% opaque minerals. The alkali feldspar and nepheline crystals are subhedral, medium to fine with habits columnar to granular, while sodalite is interstitial fine-grained. It also presents euhedral titanite grains up to 0.5 mm and enclaves with the same felsic minerals and with approximately 8% mafic minerals, including amphiboles, pyroxenes, and biotite.

Lithology 3: Porphyritic phonolite.

The porphyritic phonolite (Fig. 9C) is holocrystalline, porphyritic with a fine to very fine-grained matrix and medium- to finegrained macrocrystals of sanidine, nepheline, brown hornblende, aegirine-augite, and biotite. The mineralogy is composed of approximately 78% alkali feldspars, 7% amphibole, 5% aegirine-augite, 4% nepheline, and 3% biotite. The rock also presents titanite crystals (2%) and opaque minerals. The alkali feldspar macrocrystals are columnar, subhedral, and, in some cases, skeletal. Opaque minerals occur as dispersed crystals in the matrix and are associated with the alteration process of some grains of pyroxene, amphibole, and biotite.

Lithology 4: Trachyte.

Trachyte (Fig. 9D) is holocrystalline and has 78% of alkali feldspar, with grain size ranging from fine to very fine, amphibole (6%), clinopyroxene (5%), and biotite (4%). Crystals of titanite (2%), apatite (1%), nepheline, and opaque minerals (3%) are also present. Cancrinite, clay minerals, and carbonates are characterized as secondary minerals.

Biotite occurs as microcrystal clusters, while opaque minerals have an anhedral habit and form dispersed clusters in the matrix, assuming the habit of some alkali feldspar phenocrysts.

Lithology 5: Alkali syenite with nepheline.

This lithology (Fig. 9E) is mainly composed of 80% alkali feldspar, 10% mafic minerals (biotite, aegirina augite, and arfvedsonite), and subordinately by opaque minerals (3%), nepheline (4%), nosean, sodalite, apatite (1%), and titanite (1%), while clay minerals are secondary minerals.

Opaque minerals occur in the form of microcrystals associated with mafic minerals. The nepheline grains occur spread in the matrix. Some noseana grains measure up to 1 mm. The grains of titanite are euhedral and do not exceed 0.1 mm. There are alkali feldspar porphyries up to 5 mm. Most of the corroded edges present change to clay minerals, some with poiquilitic texture and others with micrographic texture. Most of these porphyries have Carlsbad twinning, showing a tabular habit.

Lithology 6: Mesocratic monzosyenite.

This lithology (Fig. 9F) occurs as an enclave in the alkali syenite. It is composed of 48% alkaline feldspar, 30% biotite, 8% opaque minerals, 5% pyroxene (augite), and 5% amphiboles, nepheline (2%), apatite (2%), and titanite. Opaque grains partially replaced most of the biotite grains. It features pyroxene grains (augite) with inclusions of nepheline and opaque minerals and acicular apatite of up to 2 mm. Nepheline and titanite are euhedral, while alkali feldspars are anhedral with reactions in contact with mafic minerals.

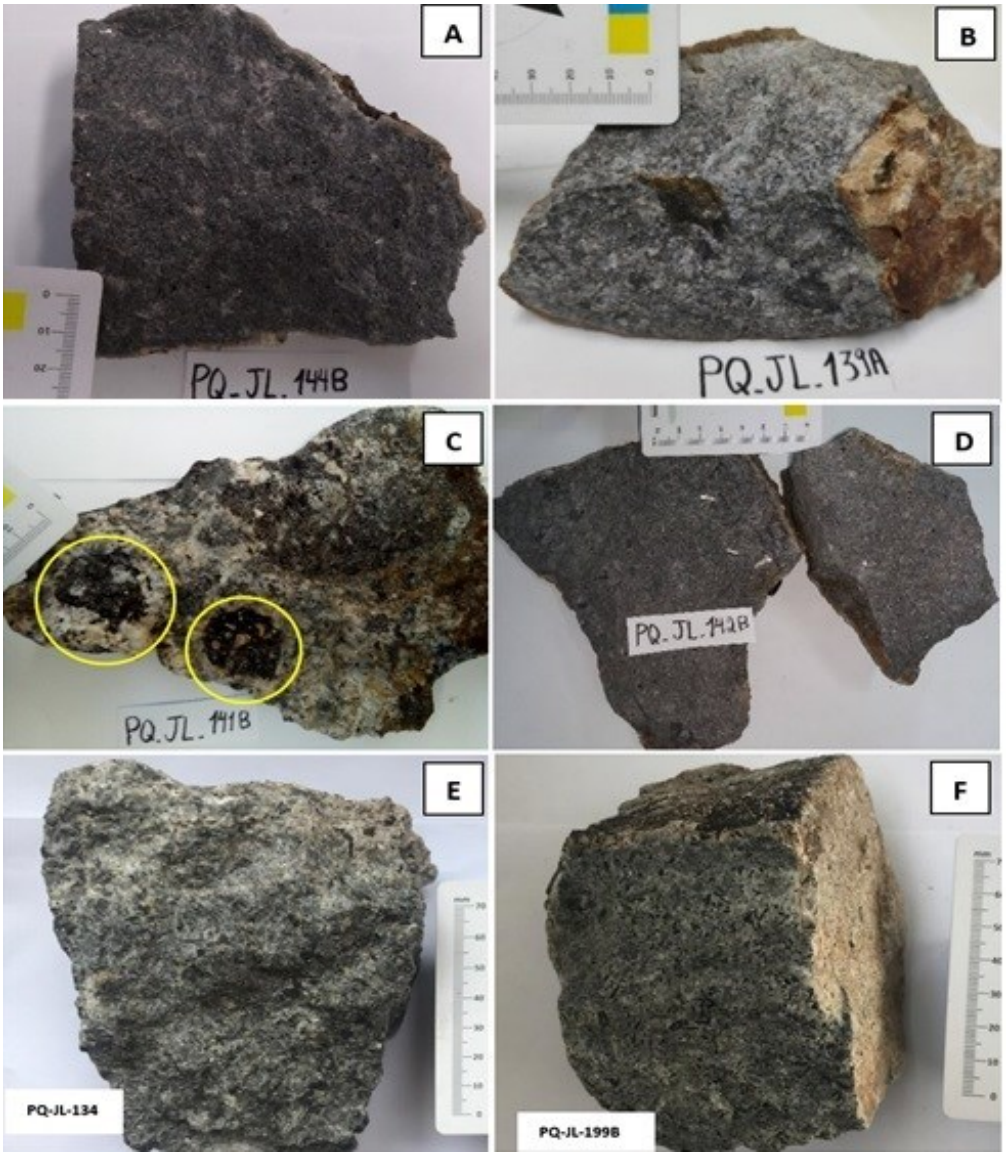

Figure 8. The image display all the lithologies observed in the field: A: Porphyritic phonolite, B: Trachyte, C: Alkali syenite with inclusions of mesocratic monzosyenite (marked by yellow circles); D: Alkali syenite with nepheline, E: Nepheline syenite and F: Alkali syenite with magnetite.

In addition to these six lithotypes, it was also possible to characterize two more widely occurring lithologies near the target area. However, the recognition of this lithology was restricted to interpretations and evidence observed in fieldwork. One of these lithologies was characterized as nepheline syenite that outcrops in the northeast portion of the studied area. The rock color is light gray, presenting at least 10% of euhedral grains of nepheline with intergranular features. It also presents euhedral titanite grains up to 0.5 mm and approximately 10% mafic minerals, including amphiboles, pyroxenes, and biotite (the latter occurs occasionally).

The other lithotype identified is an alkali syenite with magnetite, located in the south and southwest regions of the study area. The rock is light gray in color, with medium to coarse grain size (0.3–0.7 mm) and inequigranular porphyritic texture. Mafic minerals are mainly amphiboles. Alkaline feldspar porphyries measuring up to 13 mm in their longest axis have also been identified in this rock.

The presence of magnetite was verified using traditional methods applied in fieldwork. One such method involved adhering magnets to hand samples and parts of the outcrop. Two other methods used were observing the compass needle anomalous oscillation and attracting and dragging the dust removed from the samples with a magnet. Grains of titanite and biotite are also present in this rock, although they occur punctually.

From the interpretations obtained in the fieldwork and in the analysis of photomicrographs, we prepared a simplified geological map for the research region and its surroundings (Fig. 7B).

4.5.3 Lithogeochemistry

Lithogeochemical analyses processed at ACTLABS indicated a SiO_2 variable mass from 54.58 to 61.39%. This interval falls within the spectrum of intermediate composition igneous rocks (Le Maitre et al., 2002; Wilson, 1989). The MgO content varied between 0.05 and 1.58%, and according to Cox et al. (1979) and Wilson (1989), this is an indication of the rock's evolved character.

Sample 141D did not present detectable P_2O_5 values. Sc and Ni elements were significant only in some samples, and Cr was below the detection limit for all samples (Table 2).

4.5.4 Lithogeochemistry classification and series discrimination

All plutonic rock samples are located in the alkaline rock field and classified as nepheline syenite (Fig. 10A) in the total alkali vs. silica (TAS) diagram of Cox et al. (1979). Samples of subvolcanic rocks also constitute alkaline rocks and are classified as trachytes and phonolites (Fig. 10B) according to the TAS diagram (Cox et al., 1979).

We used the rare earth elements normalized for the composition of the primitive mantle according to Sun and McDonough (1989) to construct the spider diagram in Figs10C and 10D. In general, the behavior of light, medium, and heavy rare earth elements (LREE, MREE, and HREE, respectively) of plutonic and subvolcanic rocks is very similar. Both show negative P and Ti anomalies, with emphasis on sample 143B of plutonic rocks and sample 141D of subvolcanic rocks whose phosphorus did not reach the minimum limit for detection. This negative anomaly suggests a fractionation of apatite and titanite, both very well characterized in microscopic petrography and even macroscopically in the case of titanite.

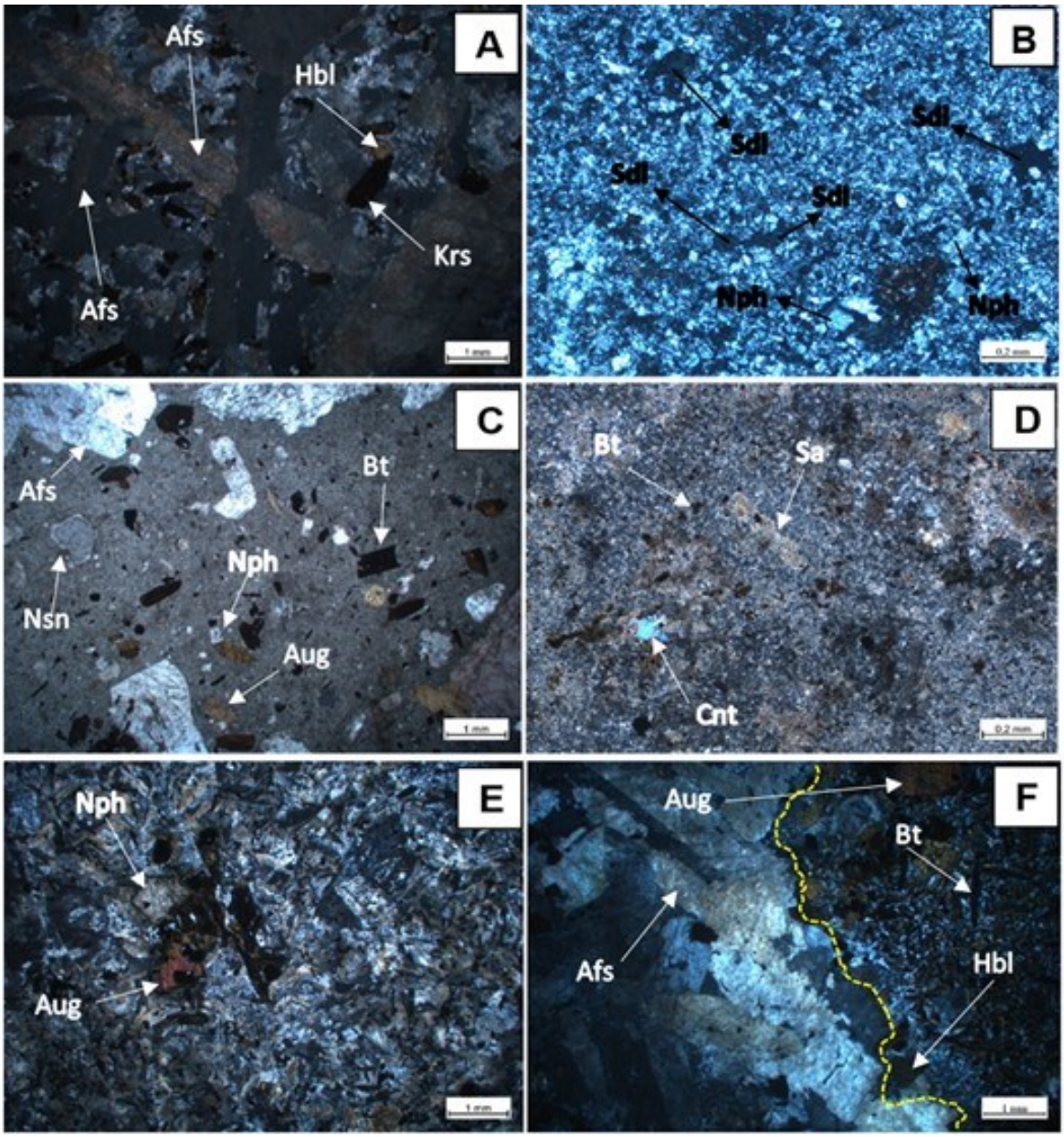

Figure 9. Photomicrograph showing the lithologies characterized in this work. A: Alkali syenite. B: Nepheline syenite with sodalite where most of the dark-colored grains are interstitial sodalite, as indicated by the arrows. C: Porphyritic phonolite. D: Trachyte. E: Alkali syenite with nepheline. F: Mesocratic monzosyenite, comprising the entire area shown to the right of the yellow dotted line. Nph: nepheline, Sdl: sodalite, Afs: alkali feldspar, Hbl: hornblende, Krs: kaersutite, Nsn: nosean, Aug: augite, Bt: biotite, Sa: sanidine, Cnt: cancrinite.

The CIPW norm (Table 3) calculation indicates the presence of quartz and normative hyperstene, which characterizes some rock samples as saturated to supersaturate in silica, despite the fact that most of the samples are silica-undersaturated, as indicated by the presence of nepheline normative. The calculation of the CIPW norm was done for both samples together and with the lithogeochemical data of the oxides recalculated for the anhydrous basis using a ratio $FeO/Fe_2O_3 = 0.50$ (Middlemost, 1989).

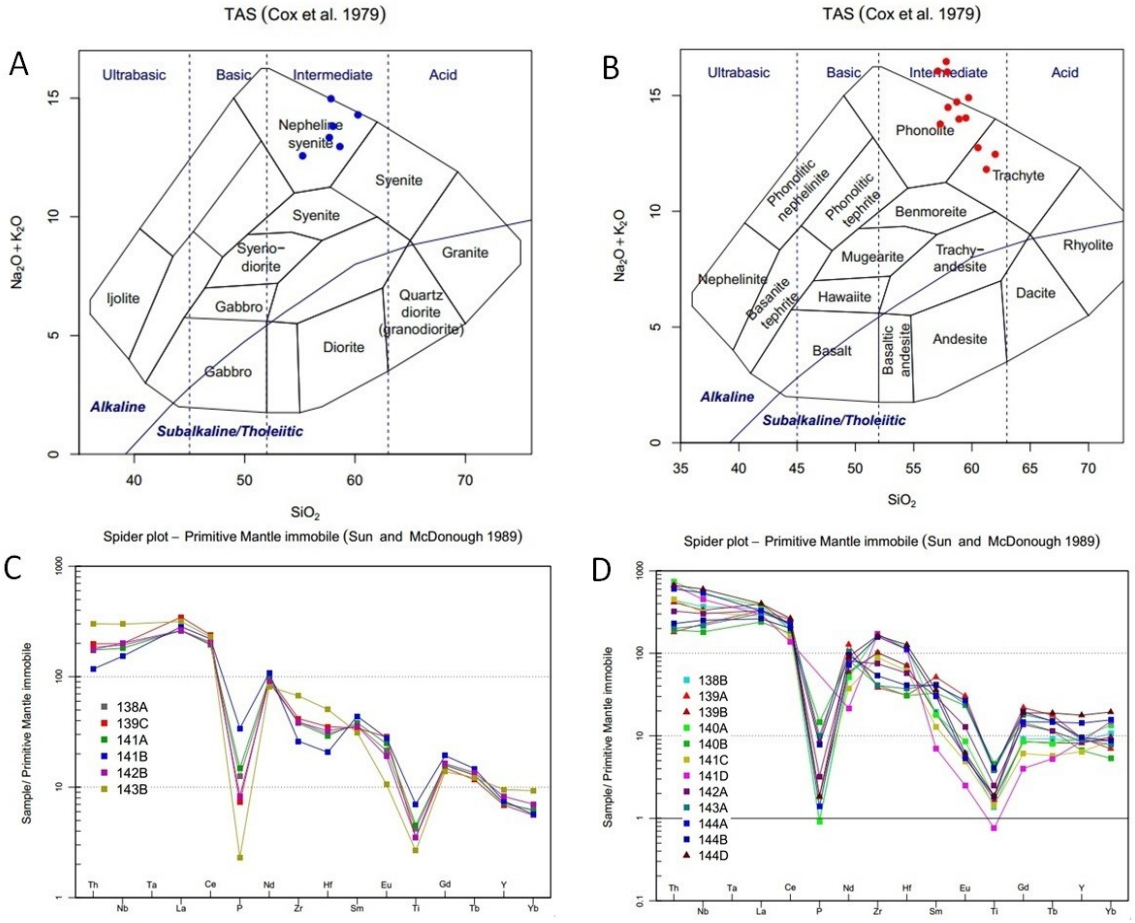

Figure 10. **A**: SiO_2 x (Na_2O + K_2O) (TAS) diagram from Cox et al. (1979) for series discrimination. Plutonic samples are- blue circles. **B**: SiO_2 x (Na_2O + K_2O) (TAS) diagram from Cox et al. (1979) for series discrimination. Subvolcanic samples are– red circles. Diagrams with trace elements of samples of plutonic rocks (**C**) and subvolcanic rocks (**D**), normalized by the primitive mantle of Sun & McDonough (1989).

The presence of acmite, as indicated by the CIPW normative calculation (Table 3), highlights the sodium nature of specific samples (138B, 141C, 141D, and 144A). This observation becomes evident by the distribution of samples in the graph of figure 11, according to the ratio Al/NK (Al_2O_3/ Na_2O+K_2O) by Al/CNK (Al_2O_3/ CaO+Na_2O+K_2O) according to Shand (1943), which shows a higher concentration of these samples in the field of peralkaline rocks and with few samples in the field of peraluminous rocks.

Most of the samples analyzed in this article have potassium affinity (Fig. 12). This characteristic was observed in other studies carried out close to the investigated area and in other alkaline intrusions present in Brazilian territory (Middlemost, 1975; Morbidelli et al., 1995; Silva et al., 2024).

Marins (2012) reports that all alkaline complexes analyzed in his scientific research presented potassic and sodic rocks, and, in contrast, ultrapotassic rocks are characterized only in the Itatiaia's alkaline complexes, Tanguá, Passa Quatro, and GericinóMendanha. Marins (2012), in the Passa Quatro Alkaline Complex, also observed the predominance of miaskitic rocks in the study area.

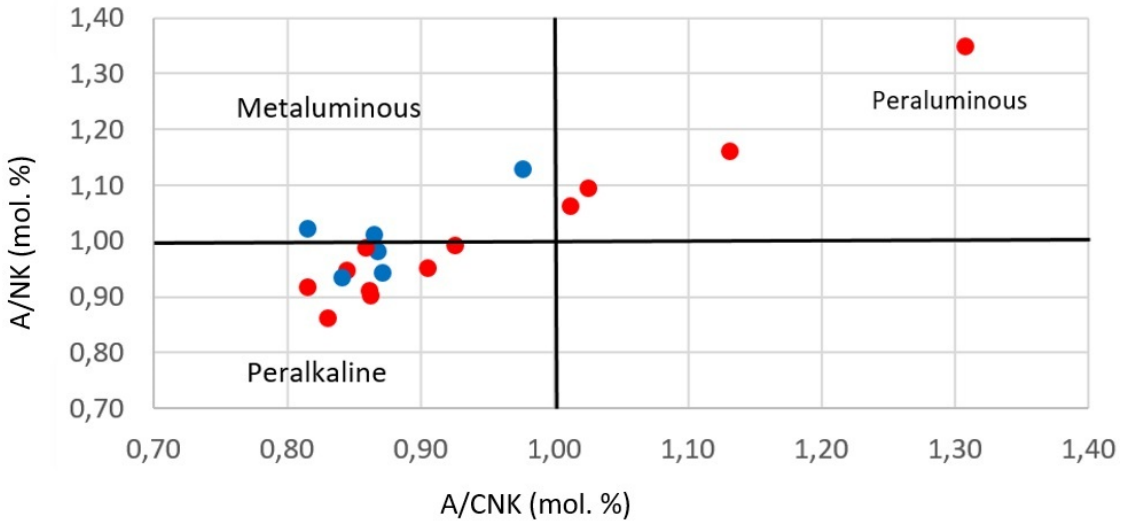

Figure 11. The diagram A/CNK X A/NK (Al_2O_3/CaO + Na_2O + K_2O X Al_2O_3/ Na_2O + K_2O (mol. %)) adapted from Shand (1943), shows the distribution of samples in the plutonic rocks represented by blue circles and subvolcanic rocks by red circles. A greater concentration of samples in the field of Peralkaline rocks is evident.

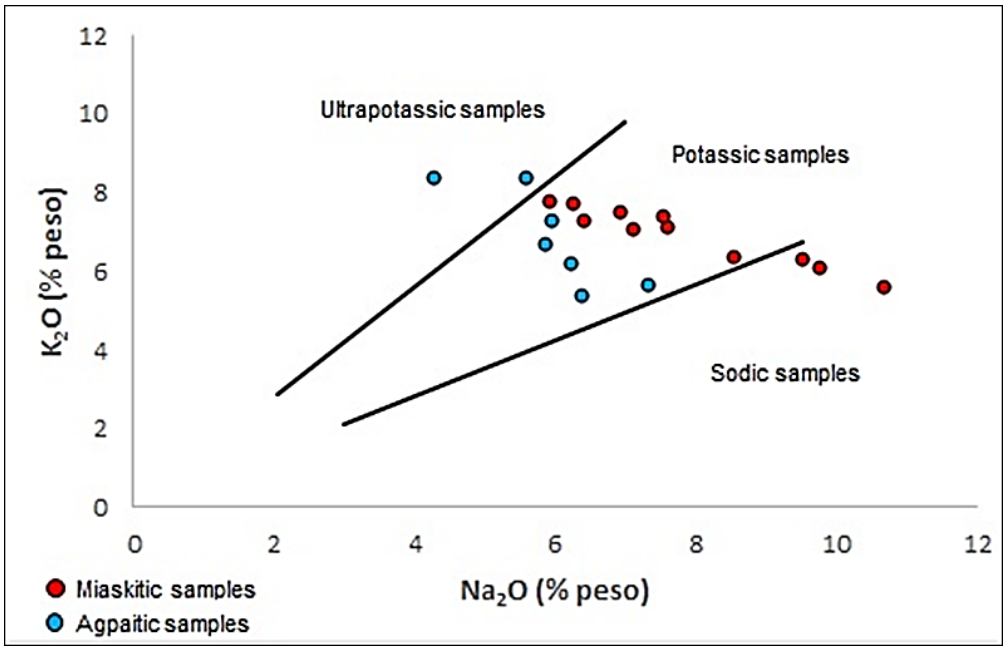

Figure 12: Discriminating diagrams of ultrapotassic, potassic and sodic suites of alkaline series, with most samples from the study area plotting in the potassic suites field. Diagram adapted from Middlemost (1975). The blue circles represent agpaitic samples, and red circles represent miaskitic samples.

4.5.5. Geochemical modeling

The study of the petrogenesis of magmatism associated with the study area would initially occur with regression analysis using the least squares method. Thus, we could construct variation diagrams, both for studies of larger elements and for incompatible mobile and immobile trace elements. In this way, it would be possible to discuss the evolutionary processes that would have occurred in the magmatic chambers during the generation of the trachytic and phonolitic bodies of the Passa Quatro Alkaline Complex.

However, the study area presented a great lithological variety of plutonic and subvolcanic rocks, and the collected samples in the fieldwork were not enough to represent all this variety in sufficient numbers for petrogenetic analyses through variation diagrams. We chose to work with partial batch melt modal modeling in order to characterize the generating source of the magmatism studied in this work. Additionally, we tested the Fractional Crystallization Model in order to assess the possibility of this evolutionary process being associated with felsic subvolcanic magmatism (from trachyte to phonolite) since there is greater representativeness in terms of the sample.

4.5.5.1 Modal batch partial melting modeling

The modal batch partial melting modeling described by the equation $C_L/C_0 = 1/F+D-FD$, according to Wood and Fraser (1976), was used to derive the composition of the generating source of the less evolved rocks from the studied region in the present article. In this equation, C_L is the concentration of a trace element in the liquid, C_0 is the concentration of a trace element in the original solid, F is the residual melt fraction, and D is the total crystal-liquid partition coefficient.

Wilson (1989) warns about the use of this and other forms of modeling (modal fractional, non-modal fractional, and nonmodal batch) pointing out that they are based on idealized assumptions and, therefore, are not much more than an attempt to approximate reality, but they are still important tools that demonstrate the application of basic principles and the limiting effects of igneous processes.

In this modeling, we consider the composition and mode of a spinel lherzolite by Maaloe and Aoki (1977), with 50% olivine, 18% orthopyroxene, 28% clinopyroxene, and 4% spinel (Table 4A). The partition coefficients used are those of basalt, calculated by Mckenzie and O'Nions (1991).

Table 4A: Adjusted mode of a spinel lherzolite according to Maaloe & Aoki (1977).

Mineral	Mode (%)	Kd-La	Kd-Yb
Olivine	0.50	0.0004	0.0015
Orthopyroxene	0.18	0.002	0.049
Clinopyroxene	0.28	0.054	0.28
Spinel	0.04	0.01	0.01
Total	1.00		

We used the concentration of La (2.06) and Yb (0.08) of the xenolith KLxm1 from the Limeira 1 Kimberlite, located 26 km north of Monte Carmelo (MG), data obtained from the work of Almeida (2009). According to the author, this xenolith is classified as a spinel lherzolite and presents high large ion lithophile element/high field strength elements (LILE/HFSE) ratios, characteristic of metasomatism provided by subduction zone fluids. The ratio of the cited La and Yb concentrations, normalized by the Thompson's chondrite (1982), reached 25.75 (Table 4B).

Table 4B: Element concentrations (ppm) and ratios of samples derived from metasomatized mantle*.

Elements	La	Yb	La/Yb**
Concentration	2.060	0.080	25.750
Normalization factor	0.329	0.22	

* According to Almeida (2009).

**La/Yb ratio normalized to chondrite of Thompson (1982).

We also used the La and Yb concentrations and the ratio between these elements (La/Yb) normalized according to Thompson's chondrites (1982) composition from the less evolved samples (trachytes, phonolites, and basanite) of this study to calculate the actual La/Yb ratios for each of these samples (Table 4C). The other data used and the results obtained are presented in Table 4D.

Table 4C: Concentrations (ppm) and element ratios of less evolved samples.

Less evolved samples	Elements		Ratio between elements
	La	Yb	La/Yb*
Saturated trachytic liquid	227	3.44	44.13
Undersaturated phonolytic liquid	211	3.83	36.84
Undersaturated tephritic liquid (PQ-GM-06D)**	87.5	2	29.26

*La/Yb ratio normalized to chondrite of Thompson (1982).

**Data from Marins (2012).

Table 4D: Data from partial melting modeling of the possible source of magmatism in the study area.

	La	D= 0,02	Yb	D= 0,09	
F	CL	CL/C0	CL	CL/C0	La/Yb*
0.01	79.48	38.58	0.82	10.26	64.76
0.02	57.61	27.97	0.75	9.38	51.33
0.03	45.77	22.22	0.69	8.68	44.06
0.04	37.16	18.04	0.64	8.01	38.77
0.05	33.96	16.49	0.62	7.71	36.81
0.06	27.42	13.31	0.56	6.99	32.80
0.07	24.25	11.77	0.53	6.57	30.85
0.08	21.73	10.55	0.50	6.20	29.30
0.09	19.69	9.56	0.47	5.87	28.04
0.10	18	8.74	0.45	5.57	27.01

F= Partial Merger percentage rate.

CL= Concentration of the element in the liquid.

C0= Trace element concentration in the source.

*La/Yb ratio normalized to Thompson chondrite (1982).

D=Total partition coefficient.

Figure 13 presents the partial melting curve of a metasomatized mantle in a melting range that varies from 0 to 10%. According to the modeling presented in this graph, with approximately 3% partial melting, it is possible to produce trachytic liquid with a La/Yb ratio equal to 44.06. The phonolytic liquid is generated with approximately 5% partial melting, presenting a La/Yb ratio of 36.81, and with approximately 8% partial melting the liquid with a tephritic composition is generated with a La/Yb ratio of 29.30 (Table 4C and 4D).

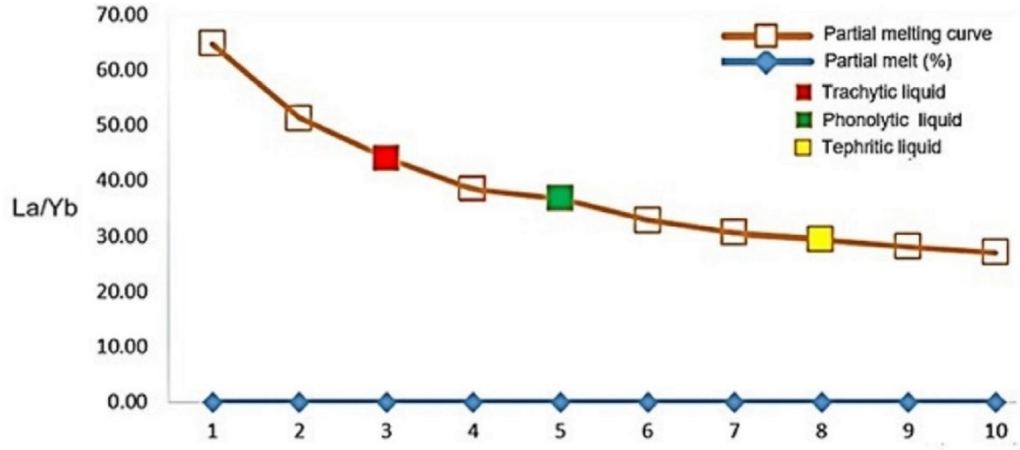

Figure 13. Graph illustrating the variation in La/Yb ratio as a function of partial melting of a metasomatized mantle, within the melting range of 0 to 10%. In this simulation, the trachytic melt (red box) is generated at approximately 3% partial melting, the phonolitic melt (green box) at approximately 5% partial melting, and the tephritic melt (yellow box) at approximately 8% partial melting.

4.5.5.2 Fractional Crystallization model

For subvolcanic rocks, the model involving fractional crystallization was the one that presented the most plausible results for the magmatic differentiation process. For this modeling, we use the Rayleigh fractionation equation: $CL/C0=F^{(D-1)}$ according to Wood and Fraser (1976).

We used partition coefficients (Kd) resulting from phenocryst-matrix analysis of evolved rocks such as panterllerite-trachyte (Mahood & Stimac, 1990), per-alkaline trachyte (Larsen, 1979), phonolite (Schnetzler & Philpotts, 1970), trachyte-basalt (villemant, 1988), trachyte (Mahood & Stimac, 1990), syenite (Marks et al., 2004), and phonolite (Olin & Wolf, 2012). There were no records of the partition coefficient of Nb for apatite, Eu for titanite, or Pr for biotite and apatite.

In general, the subvolcanic rock samples presented the following modal composition: 76% K-feldspar, 9% amphibole, 5% clinopyroxene, 4% nepheline, 3% titanite, 2% biotite, and 1% apatite (Table 5A).

Table 5A: Modal composition and Kd* of elements used in Fractional Crystallization modeling.

Mineral	Mode (%)	Kd Y	Kd Nb	Kd Yb	Kd Sm	Kd Ce	Kd Eu	Kd La	Kd Nd	Kd Hf	Kd Pr
K Feldspar	0.76	0.017	0.004	0.002	0.0004	0.0005	0.024	0.15	0.026	0.009	0.27
Nepheline	0.04	0.01	0.011	0.016	0.012	0.0011	0.043	0.01	0.013	0.008	0.013
Amphibole	0.09	0.017	1.25	0.33	0.89	2.06	1.02	2.06	0.37	7.29	0.45
Aeg-augite	0.05	1.12	0.0001	0.227	0.33	3.9	0.6	2.3	0.49	1.54	2.12
Titanite	0.03	25	5.4	13.5	0.0001	34		29	52	10	47
Biotite	0.02	0.007	0.085	0.042	0.031	0.034	0.03	0.57	0.032	0.06	
Apatite	0.01	20		10	38	30.3	30.2	39	23	0.07	
Total	1.00										
D**		1.021	0.280	0.549	0.478	1.705	0.444	1.686	1.869	1.042	1.762

* Partition Coefficient.

**Total Partition Coefficient.

For modeling, we used trace element concentrations from the most evolved sample (trachyte 139B) and the least evolved sample (phonolite 138B) among the subvolcanic rock samples (Table 5B).

Table 5B: Concentration of trace elements in the samples used in the Fractional Crystallization modeling.

Elements	Y	Nb	Yb	Ce	Sm	Eu	La	Nd	Hf	Pr
139B[a](trachyte)	37.10	238.00	4.76	386.00	8.27	0.956	273.00	80.80	22.00	34.90
138B[b](phonolite)	39.10	262.00	5.27	363.00	8.62	1,030	240.00	77.50	21.90	31.80
Enrichment rate	1.05	1.10	1.11	0.94	1.04	1.08	0.88	0.96	1.00	0.91

[a] Less evolved samples.

[b] More evolved samples.

In Table 5C, we have presented the modeled data, representing the trace element concentrations obtained by applying the data from Table 5A and Table 5B to the model, fixed at a fractional crystallization rate of 10%. Subsequently, we compared these modeled data with the actual trace element concentrations (real data) of the most differentiated sample used in the modeling process.

Table 5C: Results obtained by applying 10% Fractional Crystallization to modeling.

Elements	Y	Nb	Yb	Ce	Sm	Eu	La	Nd	Hf	Pr
Modeled CL	37.02	256.77	4.99	358.39	8.74	1.01	253.96	81.58	21.90	32.21
Real CL	39.10	262.00	5.27	363.00	8.62	1.03	240.00	77.50	21.90	31.80
% Difference	5.32	2.00	5.28	1.27	1.36	1.59	5.82	5.27	0.02	1.28
Analytical precision	7.06	11.79	5.84	5.70	6.30	3.40	6.00	6.50	0.00	4.90
Average % difference	2.90									
Average analytical precision	5.70									

4.6. Discussion

4.6.1 Petrographic aspects

In a comprehensive study of petrography and discrimination of magmatic series of PQAC rocks, Paula et al. (2019) identified the presence of two alkaline magmatic series. The first series is strongly unsaturated in silica, comprising miaskitic and agpaitic rocks. The other series is

moderately alkaline, comprising unsaturated, saturated, and supersaturated rocks in silica. Also, according to Paula et al. (2019), the predominant lithotypes are nepheline syenite, alkali syenites, and phonolites.

In our study, the alkaline magmatic series moderately unsaturated in silica predominated. Our field studies, including investigations into the textural aspects of the rocks, degree of weathering, color, optical microscopy, and geochemical analyses, led us to propose the existence of at least six distinct lithotypes.

Among these six lithotypes, four demonstrate considerable extension and are capable of mapping: trachyte, alkali syenite, alkali syenite with nepheline, and porphyritic phonolite. The remaining two lithotypes are localized occurrences found as inclusions within the mappable lithotypes: the mesocratic monzosyenite included in the alkali syenite and the nepheline syenite with sodalite occurring as inclusions in the porphyritic phonolite. Adding the lithotypes described only through fieldwork and petrography (nepheline syenite and alkali syenite with magnetite), in total there were eight lithotypes characterized in the region covered by Pico dos Três Estados and its adjacent areas.

Most lithotypes observed in this study align with the lithotypes proposed by Almeida (1983) in the Serra do Mar Alkaline Province. In general, the rock's mineralogical composition in this study is very similar to the mineralogical composition of the entire PQAC proposed by Brotzu et al. (1992). This includes a percentage of mafic minerals less than 10% by volume and a notable scarcity of plagioclase grains.

4.6.2 Possible evidence of a mingling process

The study of mixing and mingling mechanisms is crucial not only for understanding the diversity of volcanic rocks but also for understanding the entire geological scenario within the system. Both phenomena are recognized in several geological processes, each possessing distinct characteristics (Lai et al., 2008).

The occurrence or absence of these processes ultimately depends on the energy dynamics inherent to the system, specifically on the ratio between heat gain and loss. This ratio, as highlighted by Furman and Spera (1985), plays a fundamental role in determining the time required for magma mixing. Furthermore, the extent of this process and the effectiveness of mixing depend on both the intensity of convection and the viscosity ratio of the magmas involved in the process (Furman & Spera, 1985).

In addition to the globular features observed macroscopically (Figure 8C), slide petrographic analysis reveals a substantial difference in crystal granulometry between mafic and felsic materials. The granulometry of mafic material is significantly smaller than that of crystals in felsic material. This contrast arises from the temperature disparity between the materials, causing the highertemperature mafic magma to solidify more rapidly (Sklyarov & Fedorovskii, 2006). The materials' distinct mineralogical compositions involved are another factor that suggests the mingling occurrence between these two components (Lai et al., 2008).

These globular structures (Figs. 14A and 14B) and this difference in granulometry and mineralogy (Figs. 14C and 14D) observed in some samples collected in our study suggest a coexistence between two magmas with different characteristics at a given time and restricted in the magmatic chamber that gave rise to the PQAC. The volume of the mafic material is restricted to felsic and suggests that the mafic magma is subordinate to felsic magmas, which in turn dominate the magmatic chamber.

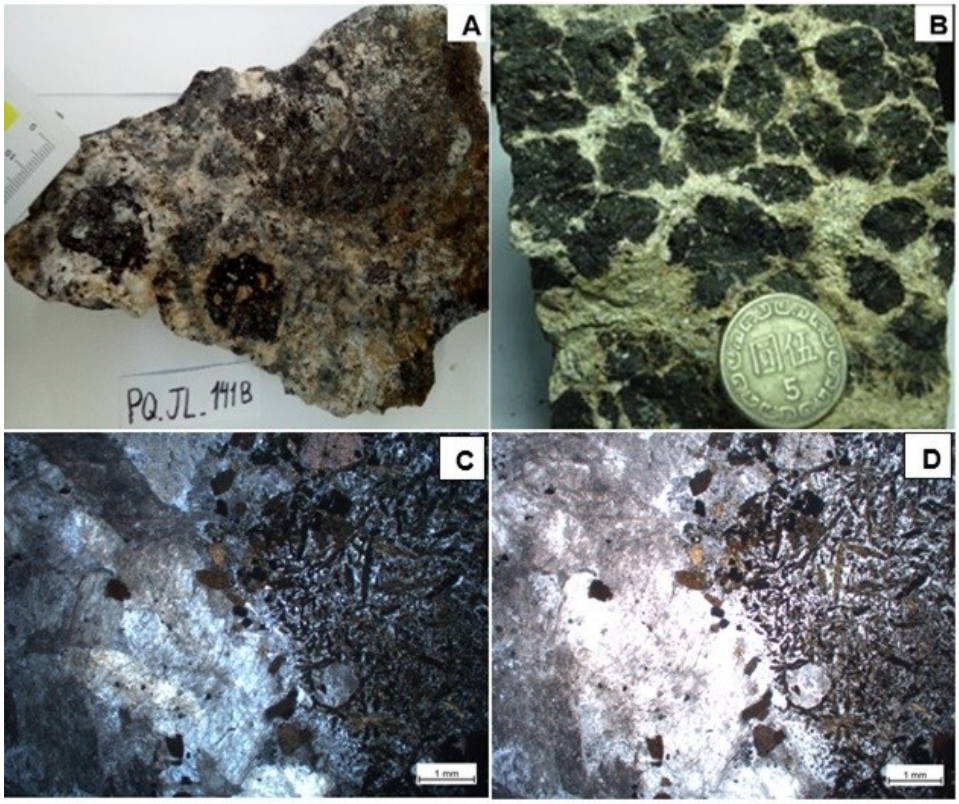

Figure 14. Spheroidal structures indicative of magma mingling processes. In panel A, we present an image of a sample collected from the study area, while panel B features an image from the work of Lai et al. (2008). Panels C and D show photomicrographs under parallel and crossed nicols, respectively, highlighting the mineralogical and granulometric differences between these two liquids.

4.6.3 Modal batch partial melting modeling

The least evolved samples in this paper presented a La/Yb ratio of 38.38 for miaskitic rocks (trachytes) and 30.51 for agpaitic rocks (phonolite). We used data from a sample of tephritic composition analyzed in previous work at PQAC (Marins, 2012), which generated a La/Yb ratio of 29.26 (Table 4C). These are very high proportions compared to the La/Yb ratio of an Oceanic Island Basalt (OIB)-type mantle, which is equal to 1.54 (Komiya et al., 2004).

When applying the La and Yb concentrations of an OIB-type mantle to partial melting modeling in modal equilibrium, we verified that it is not possible to simulate the generation of an alkaline magmatic composition with the high La/Yb ratios observed in the samples. Clague and Frey (1982) and Thompson et al. (1998) propose that an ideal range for alkaline magma generation would normally be between 0.1 and 11% of partial melting.

Thompson et al. (1998) using, REE ratios in partial melt modeling, suggest the possibility that the majority of Serra do Mar mafic magmas were generated in the range between approximately 0.1 and 1.0% partial melt from an OIB-type lherzolitic mantle containing garnet-spinel in the proportion of 70-30, respectively, at a depth of approximately 70 km from the lithosphere. In part, this explains the plagioclase absence in the samples evaluated in our study. According to Clague and Frey (1982), Honolulu volcanoes' alkaline olivine basalt and basanites

were obtained in a range ranging from 5% to approximately 11% partial melting of a lherzolitic garnet.

According to Wyllie (1987) in Comin-Chiaramonti et al. (1997), potassium magmatism is characterized by a high concentration of incompatible elements in addition to high K, which makes its genesis improbable by partial melting of conventional peridotites.

Given the aforementioned scenario, the involvement of a mantle subjected to an enrichment process becomes necessary. This could elucidate the high La/Yb ratio linked to the petrogenesis of the trachytic and phonolytic bodies within the Passa Quatro Alkaline Complex.

The enrichment of the mantle may take place in subduction zones through metasomatic processes. Comin-Chiaramonti et al. (1997), based on model ages, proposed Proterozoic metasomatic events as the catalysts for this enrichment. They argue that the gain in incompatible elements results from geodynamic processes, serving as precursor agents for the genesis of tholeiitic and alkaline magmatism in the Paraná Basin.

In this article, considering the data presented and the discussion mentioned above, we applied data from an enriched source in the La/Yb ratio to the model (Table 4B).). We work with the hypothesis that the generator mantle of alkaline magmatism analyzed in this study underwent metasomatic processes.

Most xenoliths collected in the Limeira 1 Kimberlite showed some degree of metasomatism, according to Almeida (2009). However, the KLxm1 xenolith, classified according to Streckeisen (1976) as Spinel Lherzolite, presented characteristics that fit the partial melting modeling in modal equilibrium, according to Wood and Fraser (1976).

Still, according to Almeida (2009), an important characteristic regarding the KLxm1 xenolith is the fact that it was subjected to refertilization, especially in relation to LILE, which guaranteed a high LILE/HFSE ratio, a characteristic resulting from metasomatism related to subduction zone fluids.

The range of alkaline magma generation predicted by our modeling (0–10%) is consistent with values reported in the literature. This indicates that the source of the alkaline magmatism has undergone some degree of metasomatism associated with subduction events. Such a finding supports the notion that subduction processes significantly influence the composition and characteristics of the magma source. The agreement with existing data enhances our understanding of the geochemical mechanisms driving alkaline magmatism and the implications for the geological processes at play.

4.6.4 Fractional Crystallization model

Regarding the Fractional Crystallization Model, we operate under the hypothesis that phonolites originated from a trachytic liquid composition. This proposition is aligned with Marks and Markl (2017), who suggest that agpaitic rocks result from the differentiation processes of miaskitic magmas. For Wilson (1989), phonolites may be residual liquids of undersaturated silica and intermediate alkaline differentiation series.

Applying this model, we identified a correlation between the elements Y, Nb, Yb, Ce, Sm, Eu, La, Nd, Hf, and Pr with the mineral assembly presented in table 6A, , applying 10% fractional crystallization. This correlation becomes evident when we compare the modeled liquid data with the real sample data (Table 5C).

Among the analyzed elements, only Yb, La, and Nd deviate slightly in analytical precision from the average percentage difference between the modeled liquid and PQAC

phonolite. The other elements have the average percentage difference below the average analytical precision (Table 5C). The Kd absence for certain elements in the available literature made it unfeasible to apply the model to these elements.

4.7 Conclusions

The investigation into the alkaline rock suites presented in this study has revealed a complex interplay of geological processes, particularly in relation to magma mingling and petrogenesis. Consistent with findings from similar studies, our research underscores the intricacies involved in fieldwork and the interpretation of geochemical data, which are crucial for constructing robust geological models that advance our understanding of magmatic evolution.

The integration of comprehensive field investigations with petrographic and geochemical analyses has allowed for a more nuanced characterization of subvolcanic bodies in the study area. Notably, the majority of these bodies exhibit phonolitic characteristics, with the Pico dos Três Estados region predominantly composed of porphyritic phonolitic rocks, while only a minor fraction is classified as trachyte. This detailed examination has facilitated the development of a geological map that delineates the primary facies within the target area.

Field observations of structures indicative of restricted magma mingling processes suggest the presence of a relatively stable magma chamber characterized by low convective intensity. This stability appears to have preserved the distinct compositional characteristics of the coexisting magmas within the chamber. However, further investigations are warranted to deepen our understanding of these processes and to validate their occurrence in the PQAC study area.

Modeling results indicate that the less evolved compositions observed may be associated with varying degrees of partial melting of a common mantle source. This source is distinguished by a significant enrichment in the La/Yb ratio, which exceeds that of an OIB-type source by at least 16 times. Such enrichment is likely the result of metasomatic processes, predominantly occurring during Neoproterozoic subduction events. The modeling successfully simulates the generation of alkaline magma within the range of 3 to 8% partial melting, providing insights into the magmatic processes at play.

Moreover, our application of the fractional crystallization model to the differentiation of subvolcanic bodies yielded compelling results. We propose that phonolitic bodies may originate from the differentiation of trachytic magma, beginning at approximately 10% fractional crystallization. Given the recognized lithological complexity and heterogeneity of the region, we advocate for further research to elucidate the local geological framework and to explore the implications of these findings on broader magmatic processes.

In conclusion, this study contributes significantly to the understanding of alkaline rock petrogenesis and highlights the necessity for continued exploration in this geologically rich area. The insights gained herein not only enhance our comprehension of the specific geological phenomena observed but also pave the way for future investigations that could reveal further complexities in the magmatic systems of the region.

Acknowledgments

We thank Cristiane Mara Silva da Costa, João Pedro Lopes, and Mayara Reis who gave support in the field trip and for their help in revising the English text. We also thank Actalabs for lithogeochemical analyses. We, in particular, are extremely grateful to the PETROMAGMATISM project (FAPUR 19/03 and SAP 4600581919—authorized by the National Agency of Petroleum, Natural Gas, and Biofuels of Brazil) that supported this research.

Disclosure statement

The authors of this work did not report any potential conflict of interest.

How to cite: Freitas, G. C., Corval, A., Silva, J. C. L., Pinheiro, H. S. K., & Valente, S. C. (2024). Subvolcanic petrology of the Pico dos Três Estados region (SE Brazil): Implications for Alkaline Magmatic Evolution. *Brazilian Journal of Geology*, *54*(2), e20240009. https://doi.org/10.1590/2317-4889202420240009

G.C.F.: Conceptualization, Data curation, Formal analysis, Investigation, Methodology, Project administration, Software, Validation, Visualization, Writing—original draft, Writing—review and editing. A.C.: Conceptualization, Data curation, Formal analysis, Investigation, Methodology, Project administration, Resources, Software, Supervision, Validation, Visualization, Writing—original draft, Writing—review and editing. J.C.L.S.: Conceptualization, Data curation, Formal analysis, Investigation, Methodology, Software, Supervision, Validation, Visualization, Writing—original draft, Writing—review and editing. S.C.V.: Conceptualization,

Data curation, Formal analysis, Funding acquisition, Investigation, Methodology, Project administration, Resources, Supervision, Validation, Visualization, Writing—original draft, Writing—review and editing. H.S.K.P.: Formal analysis, Methodology, Software, Supervision, Validation, Visualization.

Competing interests: The authors declare no competing interests.

Address for access to supplementary material:

https://doi.org/10.5281/zenodo.13251591

4.8 References

Almeida, F.F.M., 1983. Relações tectônicas das rochas alcalinas mesozóicas da região meridional da Plataforma Sul Americana: **Revista Brasileira de Geociências**, v. 13, p. 139–158.

Almeida, F.F.M., 1991. O alinhamento magmático de Cabo Frio, in Simpósio de Geologia do Sudeste (2nd): São Paulo, Atas, p. 423–428.

Almeida, V.V., 2009. Mineralogia e petrologia de xenólitos mantélicos das regiões de Ubatuba (SP) e Monte Carmelo (MG): evidências de fusão parcial e metassomatismo no manto superior do sudeste brasileiro [M.Sc. dissertation]: Programa de pós-graduação em Mineralogia e Petrologia. Universidade de São Paulo. Instituto de Geociências, P. 153.

Best, M.G., 2002. Igneous and Metamorphic Petrology: 2nd ed. Wiley-Blackwell, p. 752.

Brotzu, P., Barbieri, M., Beccaluva, L., Garbarino, C., Gomes, C.B., Macciotta, G., Melluso, L., Morbidelli, L., Ruberti, E., Sigolo, J. B., and Traversa, G., 1992. Petrology and geochemistry of the Passa Quatro alkaline complex, southeastern Brazil: Journal of South American Earth Sciences, v. 6, no. 4, p. 237–252.

Chiessi, C.M., 2004. Tectônica Cenozóica do Maciço Alcalino de Passa Quatro (SP-MG-RJ) [M.Sc. dissertation]: Instituto de Geociências, Universidade de São Paulo, São Paulo, 116 p.

Clague, D.A., Frey, F.A., 1982. Petrology and Trace Element Geochemistry of the Honolulu Volcanics, Oahu: Implications for the Oceanic Mantle below Hawaii. Journal of Petrology, v. 23, p. 447–504.

Cox, K.G., Bell, J.D., Pankhurst, R.J., 1979. The interpretation of igneous rocks. London: George Allen & Unwin. 450p.

Comin-Chiaramonti, P., Cundari, A., Piccirillo, E.M., Gomes, C.B., Castorina, F., Censi, P., De Min, A., Marzoli, A., Speziale, S., Velázquez, V.F., 1997. Potassic and sodic igneous rocks from Eastern Paraguay: their origin from the lithospheric mantle and genetic relationships with the associated Parana flood tholeiites. Journal of Petrology, v. 38, p. 495–528.

Furman, T., and Spera, F.F., 1985. Co-mingling of acid and basic magma with implications for the origin of mafic I-type xenoliths: field and petrochemical relations of an unusual dike complex at Eagle Lake, Sequoia National Park, California, U.S.A. In: B. H. Baker and A. R. McBirney (Editors), Processes in Magma Chambers. J. Volcanol. Geotherm, v. 24, Issue 1–2, p. 151–178.

Gill, R., 2014. Rochas e Processos Ígneos. Um guia prático: Porto Alegre: Bookman, Issue 1, p. 502.

Google Earth (2021). Passa Quatro Alkaline Complex Location. Image Landsat/Copernicus. Retrieved from https://earth.google.com.

Guarino, V., Gennaro, R., Melluso, L., Ruberti, E., and Azzone, R., 2019. The transition from miaskitic to agpaitic rocks, as highlighted by the accessory phase assemblages in the Passa Quatro alkaline complex (southeastern Brazil: The Canadian Mineralogist, v. 57, p. 339–361.

Heilbron, M., Silva, L.G.E., Almeida, J.C.H., Tipinambá, M., Peixoto, C., Valeriano, C.M., Rodrigues, S.W.O., Ragatky, C.D., Silva, M.A., Monteiro, T., Freitas, N.C., Miguens, D., and Girão, R., 2020. Proterozoic to Ordovician geology and tectonic evolution of Rio de Janeiro state, SE-Brazil: Insights on the central Ribeira orogen from the new 1: 400,000 scale geologic map: Brazilian Journal of Geology, v. 50, number 2.

Hibbard, M.J. 1995. Petrography to petrogenesis, Prentice Hall, Englewood Cliffs, New Jersey, p. 587.

Instituto Brasileiro de Geografia e Estatística (IBGE) (1974). Folha Topográfica do Município de Passa Quatro. Sup. Cartografia do IBGE, Esc. 1:50.000, folha SF-23-Z-A-I-3. IBGE.

Janousek, V., Farrow, C.M., Erban, V., 2006. Interpretation of Whole-rock Geochemical Data in Igneous Geochemistry: Introducing Geochemical Data Toolkit (GCDkit). Journal of Petrology, volume 47, number 6, p. 1255–1259.

Komiya, T., Maruyama, S., Hirata, T., Yurimoto, H., & Nohda, S. (2004). Geochemistry of the oldest MORB and OIB in the Isua Supracrustal Belt, southern West Greenland: Implications for the composition and temperature of early Archean upper mantle. The Island Arc, 13(1), 47-72. https://doi.org/10.1111/j.1440-1738.2003.00416.x

Lai, Y., Song, S., Lizuka, Y., 2008. Magma mingling in the Tungho area, Coastal Range of eastern Taiwan. Journal of Volcanology and Geothermal Research 178, p. 608-623.

Larsen, L.M., 1979. Distribution of REE and other trace elements between phenocrysts and peralkaline undersaturated magmas, exemplified by rocks from the Gardar igneous province, south Greenland: Lithos, v. 12, p. 303–315.

Le Maitre, R.W., Bateman, P., Ducek, A., Keller, J., Lameyre, J., Le Bas, M.J., Sabine, P.A., Schmid, R., Sorensen, H., Streckeisen, A., Wooley, A.R. Zanettin, B., 2002. A classification of igneous rocks and glossary of term: Blackwell Scientific Pub, London, 193 p.

Lechler, P.J., and Desilets, M.O., 1987. A review of the use of loss on ignition as a measurement of total volatiles in whole-rock analysis: Chem. Geol., v. 63, p. 341–344.

Maaloe, S., and Aoki, K., 1977. The Major Element composition of the upper mantle estimated from the composition of lherzolites: Contributions to Mineralogy and Petrology, v. 63, p.161–173.

Mackenzie, W.S., Donaldson, C.H., and Guilford, C., 1982. Atlas of igneous rocks and their textures: New York, John Wiley & Sons, Inc, p. 148.

Mahood, G. A., & Stimac, J. A. (1990). Trace-element partitioning in pantellerites and trachytes. Geochimica et Cosmochimica Acta, 54(8), 2257-2276. https://doi.org/10.1016/0016-7037(90)90050-U

Marins, G.M., 2012. Estudo do magmatismo máfico de complexos alcalinos do Sudeste do Brasil (Dissertação de Mestrado): Rio de Janeiro, Universidade do Estado de Rio de Janeiro, Centro de Tecnologia e Ciências, Faculdade de Geologia, p.161.

Marks, M., Halama, R., Wenzel, T., Markl, G., 2004. Trace element variations in clinopyroxene and amphibole from alkaline to peralkaline syenites and granites: implications for mineral–melt trace-element partitioning. Chem. Geol., v. 211, p.185-215.

Marks, M.A.W., and Markl, G., 2017. A global review on agpaitic rocks: Earth Science Review, v. 173, p. 229–258.

McKenzie, D., & O'Nions, R. K. (1991). Partial melt distributions from inversion of rare earth element concentrations. Journal of Petrology, 32(5), 1021-1091. https://doi.org/10.1093/petrology/32.5.1021

McKenzie, D., and O'Nions R.K., 1991. Partial melt distributions from inversion of rare earth element concentrations. J. Petrology, v. 32, p. 1021–1091.

Middlemost, E.A.K., 1975. The basalt clan: Earth Science Review, v. 11, p. 337–364.

Middlemost, E.A., 1989. Iron oxidation ratios, norms and the classification of volcanic rocks: Chemical Geology, v. 77, p. 19–26.

Montes-Lauar, C.R., Pacca, I.G., Melfi, A.J., Kawashita, K., 1995. Late Cretaceous alkaline complexes, southeastern Paleomagnetism and geochronology. Earth and Planetary Science 134 (1995) p. 425–440.

Morbidelli, L., Gomes, C.B., Beccaluva, L., Brotzu, P., Conte, A.M., Ruberti, E., and Traversa, G., 1995. Mineralogical, petrological and geochemical aspects of alkaline and alkaline-carbonatite associations from Brazil: Earth Science Review, v. 39, number. 3–4, p. 135–168.

Olin, P.H., Wolf, J.A., 2012. Partitioning of rare earth and high field strength elements between titanite and phonolitic liquid. Lithos, v. 128-131, p. 46–54.

Paula, L.T., Santos, Y.D., Lopes, J., Freitas, G.C, Corval, A., Neysi, C., Valente, S.C., 2019. 'Petrografia e série magmáticas do complexo alcalino Passa Quatro (RJ-MG-SP), sudeste do Brasil: Anais do 16º simpósio de geologia do sudeste, p. 314.

Riccomini, C., Velázquez, V.F., Gomes, C.B., 2005. Tectonic controls of the Mesozoic and Cenozoic alkaline magmatism in central-southern Brazilian Plataform. In: Comin-Chiaramonti P. and Gomes C.B. (eds.), Mesozoic to Cenozoic alkaline magmatism in the Brazilian Platform. São Paulo, EDUSP-FAPESP, p. 31–56.

Rollinson, H. R. (1993). Using geochemical data: evolution, presentation, interpretation. Longman Scientific and Technical.

Rollinson, H. R., & Pease, V. (2021). using geochemical data: to understand geological processes (2nd ed.). Cambridge University Press.

Schnetzler, C.C. and Philpotts, J.A., 1970. Partition coefficients of rare-earth elements between igneous matrix material and rock-forming mineral phenocrysts: II. Geochimica et Cosmochimica Acta, v. 34, number 3, p. 331–340.

Shand, S.J., 1943. Eruptive rocks. Their genesis, composition, classification, and their relation to ore-deposits with a chapter on meteorite: New York, John Wiley & Sons.

Sigolo, J.B., 1988. As formações bauxíticas lateríticas do maciço alcalino de Passa Quatro, MG [Ph.D. thesis]: São Paulo, São Paulo University, p. 186.

Sigolo, J.B., Ruberti, E., Gomes, C.B., 1992. O complexo alcalino de Passa Quatro: dados geológicos preliminares. Boletim IG-USP, v. 12, p. 109–112.

Silva, J.C.L., Valente, S.C., Almeida, C.N., 2022. Phonolitic ring dike and plug in the Passa Quatro alkaline complex: undercooling induced by devolatilization as evidence for volcanism; Proceedings of the VIII symposium on volcanism and associated environments, p. 58.

Silva, J.C.L., Valente, S.C., Almeida, S. N., Marins, G. M., 2024. The origin of the Daly gap by fractional crystallization in a transcrustal plumbing system in the Passa Quatro alkaline complex (SE Brazil), International Geology Review, p. 25.

Sklyarov, E.V., Fedorovskii, V.S., 2006. Magma mingling: Tectonic and geodynamic implications. Geotectonics, v. 40, number. 2, p. 120–134.

Sonoki, I.K., and Garda, G.M., 1988. Idades K-Ar de rochas alcalinas do Brasil meridional e Paraguai Oriental: compilação e adaptações às novas constantes de decaimento: Boletim de Geociências do IGc-USP Série Científca, v. 19, p. 63–85.

Streckeisen, A.L., 1976. Classification of the common igneous rocks by means of their chemical composition: a provisional attempt. Neus Jahrbuch fur Mineralogie, Monatshefte, v.1, p. 1–15.

Sun, S.-S., & McDonough, W. F. (1989). Chemical and isotopic systematics of oceanic basalts: implications for mantle composition and processes. In: Saunders, A. D., & Norry, M. J. (eds.), Magmatism in the ocean basins. Geological Society of London, Special Publication, 42, 313-345. https://doi.org/10.1144/GSL.SP.1989.042.01.19

Thompson, R.N., 1982. Magmatism of the British tertiary volcanic province: Scottish Journal of Geology, v. 18, no. 1, p. 49–107.

Thompson, R.N., Gibson, S.A., Mitchell, J.G., Dickin, A.P., Leonardos, O.H., Brod, J.A., Greenwood, J.C., 1998. Migrating Cretaceous–Eocene Magmatism in the Serra do Mar alkaline province, SE Brazil: Melts from the deflected Trindade mantle plume?: Journal of Petrology, v. 39, p. 1493–1526.

Ulbrich, H.H.G.J., and Gomes, C.B., 1981. Alkaline rocks from continental Brazil: Earth Science Review, v. 17, number. 1–2, p. 135–154.

Valente, S.C., Ellan, R.M., Fallick, A.E., Meighan, I.G., 2002. The assessment of post-magmatic processes in the Serra do Mar dyke swarm, SE Brazil: proposals for acid leaching techniques and criteria for petrogenetic interpretations. Ver. Univ. Rural., Sér. Ciênc. Exatas e da Terra, v. 21, number. 1, p.1–20.

Villemant, B., 1988. Trace element evolution in the Phlegrean Fields (Central Italy): fractional crystallization and selective enrichment. Laboratoire de Geochimie Comparee et Systematique, UPMC and CNRS UA 196, 4 Place Jussieu, F-75005 Paris, France. Contrib Mineral Petrol, v. 98, p. 169–183.

Zalán, P.V. and Oliveira, J.A.B. 2005. 'Origin and structural evolution of the Cenozoic Rift System of Southeastern Brazil', Petrobras Geosciences Bulletin, v. 13, number. 2, p. 269–300.

Wilson, M., 1989. Igneous petrogenesis: London, Unwin Hyman, p. 466.

Wood, B.J., and Fraser, D.G., 1976. Elementary Thermodynamics for Geologists: Oxford, Oxford University Press, p.318.

Wyllie, P.J., 1987. Volcanic rocks: boundaries from experimental petrology. Fortschritte der Mineralogie, v. 65, p. 249–28

5 CONCLUSÕES E TRABALHOS FUTUROS

Foi possível fazer uma caracterização petrológica da área de estudo integrando trabalho de campo, petrografia e com auxílio do estudo geoquímico. Essa integração de estudos possibilitou a reclassificação litológica da formação rochosa que sustenta o Pico dos Três Estados, que se trata de um fonolito porfirítico. Corpos traquíticos também foram caracterizados, porém, em uma proporção bem menor com relação à ocorrência de fonolitos.

Além desses corpos subvulcânicos, também foram caracterizadas outras faciologias. Ambas foram reunidas em um mapa geológico que proporcionou uma maior riqueza de detalhes da área estudada.

Os resultados da modelagem sugerem que as composições menos evoluídas na área podem estar ligadas a diferentes graus de fusão parcial da mesma fonte mantélica. Uma característica desta fonte é o seu enriquecimento na razão La/Yb, enriquecimento que pode estar associado a processos de metassomatização resultantes de eventos sucessivos de subducção ocorridos no Neoproterozóico.

A aplicação do modelo de cristalização fracionada na diferenciação de corpos subvulcânicos apresentou resultados satisfatórios, propomos que os corpos fonolíticos podem ser gerados através da diferenciação de líquidos traquíticos.

As estruturas indicativas de processo de mistura de magmas devem ser investigadas com mais detalhes em estudos posteriores. Um número maior de amostras deve ser coletado, o que possibilitaria isolar cada uma das litologias e estuda-las, isoladas e conjuntamente, com o objetivo de se estabelecer a relação entre elas e confirmar, se realmente trata-se de processos de mingling. Além disso, toda a área estudada apresentou uma complexidade e heterogeneidade faciológica muito importante, por isso, defendemos mais investigações nesta região para melhorar a nossa compreensão da geologia local.

6 REFERÊNCIAS BIBLIOGRÁFICAS

Almeida, F.F.M. O alinhamento magmático de Cabo Frio. **In Simpósio de Geologia do Sudeste** (2nd): São Paulo, Atas, p. 423-428, 1991.

Best, M.G. **Igneous and Metamorphic Petrology**: 2nd ed. Wiley-Blackwell, p. 752, 2002.

Brotzu, P., Barbieri, M., Beccaluva, L., Garbarino, C., Gomes, C.B., Macciotta, G., Melluso, L., Morbidelli, L., Ruberti, E., Sigolo, J. B., and Traversa, G. Petrology and geochemistry of the Passa Quatro alkaline complex, southeastern Brazil: **Journal of South American Earth Sciences**, v. 6, no. 4, p. 237-252, 1992.

Chiessi, C.M. **Tectônica Cenozóica do Maciço Alcalino de Passa Quatro (SP-MG-RJ)** (dissertação): Instituto de Geociências, Universidade de São Paulo, São Paulo, p.116, 2004.

Gill, R. **Rochas e Processos ígneos. Um guia prático**: Porto Alegre: Bookman, Issue 1, p. 502, 2014.

Guarino, V., Gennaro, R., Melluso, L., Ruberti, E., and Azzone, R. The transition from miaskitic to agpaitic rocks, as highlighted by the accessory phase assemblages in the Passa Quatro alkaline complex (southeastern Brazil: **The Canadian Mineralogist**, v. 57, p. 339-361, 2019.

Heilbron, M., Silva, L.G.E., Almeida, J.C.H., Tipinambá, M., Peixoto, C., Valeriano, C.M., Rodrigues, S.W.O., Ragatky, C.D., Silva, M.A., Monteiro, T., Freitas, N.C., Miguens, D., and Girão, R. Proterozoic to Ordovician geology and tectonic evolution of Rio de Janeiro state, SE-Brazil: Insights on the central Ribeira orogen from the new 1: 400,000 scale geologic map: **Brazilian Journal of Geology**, v. 50, number 2, 2020.

IBGE. **Folha Topográfica do Município de Passa Quatro**. Sup. Cartografia do IBGE, Esc. 1:50.000, folha SF-23-Z-A-I-3, 1974.

Hibbard, M.J. **Petrography to petrogenesis**, Prentice Hall, Englewood Cliffs, New Jersey, p. 587, 1995.

Janousek, V., Farrow, C.M., Erban, V. Interpretation of Whole-rock Geochemical Data in Igneous Geochemistry: Introducing Geochemical Data Toolkit (GCDkit). **Journal of Petrology**, volume 47, number 6, p. 1255-1259, 2006.

Le Maitre, R.W., Bateman, P., Ducek, A., Keller, J., Lameyre, J., Le Bas, M.J., Sabine, P.A., Schmid, R., Sorensen, H., Streckeisen, A., Wooley, A.R. Zanettin, B. **A classification of igneous rocks and glossary of term**: Blackwell Scientific Pub, London, 193 p, 2002.

Lechler, P.J., and Desilets, M.O. A review of the use of loss on ignition as a measurement of total volatiles in whole-rock analysis: **Chem. Geol**., v. 63, p. 341-344, 1987.

Mackenzie, W.S., Donaldson, C.H., and Guilford, C. **Atlas of igneous rocks and their textures**: New York, John Wiley & Sons, Inc, p. 148, 1982.

Marins, G.M. **Estudo do magmatismo máfico de complexos alcalinos do Sudeste do Brasil** (Dissertação): Rio de Janeiro, Universidade do Estado de Rio de Janeiro, Centro de Tecnologia e Ciências, Faculdade de Geologia, p.161, 2012.

Montes-Lauar, C.R., Pacca, I.G., Melfi, A.J., Kawashita, K. Late Cretaceous alkaline complexes, southeastern Paleomagnetism and geochronology. **Earth and Planetary Science** 134, p. 425-440, 1995.

Morbidelli, L., Gomes, C.B., Beccaluva, L., Brotzu, P., Conte, A.M., Ruberti, E., and Traversa, G. Mineralogical, petrological and geochemical aspects of alkaline and alkaline-carbonatite associations from Brazil: **Earth Science Review**, v. 39, number. 3-4, p. 135-168, 1995.

Riccomini, C., Velázquez, V.F., Gomes, C.B. Tectonic controls of the Mesozoic and Cenozoic alkaline magmatism in central-southern Brazilian Plataform. In: Comin-Chiaramonti P. and Gomes C.B. (eds.), Mesozoic to Cenozoic alkaline magmatism in the Brazilian Platform. **São Paulo, EDUSP-FAPESP**, p. 31-56, 2005.

Sigolo, J.B. **As formações bauxíticas lateríticas do maciço alcalino de Passa Quatro, MG** (Tese): São Paulo, São Paulo University, p. 186, 1988.

Sigolo, J.B., Ruberti, E., Gomes, C.B. O complexo alcalino de Passa Quatro: dados geológicos preliminares. **Boletim IG-USP**, v. 12, p. 109-112, 1992.

Silva, J.C.L., Valente, S.C., Almeida, C.N. Phonolitic ring dike and plug in the Passa Quatro alkaline complex: undercooling induced by devolatilization as evidence for volcanism; **Proceedings of the VIII symposium on volcanism and associated environments**, p. 58, 2022.

Silva, J.C.L., Valente, S.C., Almeida, S. N., Marins, G. M. The origin of the Daly gap by fractional crystallization in a transcrustal plumbing system in the Passa Quatro alkaline complex (SE Brazil), **International Geology Review,** p. 25, 2024.

Sonoki, I.K., and Garda, G.M. Idades K-Ar de rochas alcalinas do Brasil meridional e Paraguai Oriental: compilação e adaptações às novas constantes de decaimento: **Boletim de Geociências do IGc-USP Série Científca**, v. 19, p. 63-85, 1988.

Thompson, R.N., Gibson, S.A., Mitchell, J.G., Dickin, A.P., Leonardos, O.H., Brod, J.A., Greenwood, J.C. Migrating Cretaceous–Eocene Magmatism in the Serra do Mar alkaline province, SE Brazil: Melts from the deflected Trindade mantle plume?: **Journal of Petrology**, v. 39, p. 1493-1526, 1998.

Ulbrich, H.H.G.J., and Gomes, C.B. Alkaline rocks from continental Brazil: **Earth Science Review**, v. 17, number. 1–2, p. 135-154, 1981.

Valente, S.C., Ellan, R.M., Fallick, A.E., Meighan, I.G. The assessment of post-magmatic processes in the Serra do Mar dyke swarm, SE Brazil: proposals for acid leaching techniques and criteria for petrogenetic interpretations. **Ver. Univ. Rural., Sér. Ciênc. Exatas e da Terra**, v. 21, number. 1, p.1-20, 2002.

Zalán, P.V. and Oliveira, J.A.B. 'Origin and structural evolution of the Cenozoic Rift System of Southeastern Brazil', **Petrobras Geosciences Bulletin**, v. 13, number. 2, p. 269-300, 2005.

Wilson, M. **Igneous petrogenesis**: London, Unwin Hyman, p. 466, 1989.

7 ANEXOS

Tabela 1: Resultados estatísticos analíticos de dados litogeoquímicos de dezoito amostras da área de estudo. DP: Desvio Padrão; CV: Coeficiente de Variação; NA: Número de Amostras; DL: Limite de Detecção (continua).

Elementos	Mínimo	Máximo	Média	DP	CV	NA	LD
SiO_2	54.58	61.39	57.75	1.92	0.03	18	0.01
TiO_2	0.16	1.51	0.66	0.34	0.51	18	0
Al_2O_3	19.09	23.48	20.82	1.07	0.05	18	0.01
$Fe_2O_3^T$	1.99	5.45	3.03	0.76	0.25	18	0.01
MnO	0.17	0.39	0.25	0.07	0.28	18	0
MgO	0.05	1.58	0.44	0.37	0.83	18	0.01
CaO	0.37	3.5	1.48	0.84	0.57	18	0.01
Na_2O	4.25	10.65	7.08	1.63	0.23	18	0.01
K_2O	5.4	8.42	6.93	0.92	0.13	18	0.01
P_2O_5	0.02	0.74	0.17	0.18	1.07	17	0.01
LOI	0.62	4.22	1.73	1.11	0.64	18	
Total	99.65	100.76	100.32	0.36	0	18	0.01

Tabela 1: Continuação

Elemento	Mínimo	Máximo	Média	DP	CV	NA	LD
Sc	1	5	2.17	0.94	0.43	12	1
Ni	20	40	25	10	0.4	4	20
Cr						nd	20
Co	6	17	10.17	3.22	0.32	18	1
V	6	82	24.83	17.8	0.72	18	5
Ba	2	898	200.67	243.19	1.21	18	2
Rb	101	363	189.28	73.51	0.39	18	1
Sr	3	1816	611	636.18	1.04	18	2
Y	29.3	80.9	41.16	12.74	0.31	18	0.5
Zr	292	1915	905.33	582.52	0.64	18	1
Nb	109	428	219.28	97.95	0.45	18	0.2
La	165	274	214.94	33.41	0.16	18	0.05
Ce	244	471	372.94	56.91	0.15	18	0.05
Pr	16.3	54.1	38.91	9.23	0.24	18	0.01
Nd	29.3	173	108.63	35.89	0.33	18	0.05
Sm	3.13	22.9	13.8	5.17	0.37	18	0.01
Eu	0.42	5.11	2.7	1.67	0.62	18	0.01
Gd	2.4	13.1	8.41	2.97	0.35	18	0.01
Tb	0.57	2.04	1.31	0.41	0.31	18	0.01
Dy	4.06	13	7.62	2.2	0.29	18	0.01
Ho	0.95	2.87	1.53	0.46	0.3	18	0.01
Er	3.23	8.62	4.64	1.37	0.29	18	0.01
Tm	0.42	1.4	0.69	0.25	0.37	18	0.01
Yb	2.63	9.58	4.65	1.96	0.42	18	0.01
Lu	0.38	1.43	0.72	0.32	0.45	18	0
Hf	6.4	39.2	18.28	10.74	0.59	18	0.1
Pb	7	46	20	10.8	0.54	18	5
Th	9.97	62.9	29.62	17.25	0.58	18	0.05
U	1.73	15.8	5.6	3.56	0.64	18	0.01

Tabela 2: Dados litogeoquímicos da área de estudo: elementos maiores em % em peso, elementos traços e elementos de terras raras em ppm (continua).

	Rochas Subvolcanicas												Rochas Plutonicas					
	138B	**139A**	**139B**	**140A**	**140B**	**141C**	**141D**	**142A**	**143A**	**144A**	**144B**	**144D**	**138A**	**139C**	**141A**	**141B**	**142B**	**143B**
SiO_2	55.98	59.22	60.44	58.66	56.28	54.58	55.72	58.6	57.26	59.57	58.67	61.39	56.69	58.51	56.39	54.73	57.52	59.21
TiO_2	0.3	0.84	0.36	0.39	1	0.31	0.16	0.54	0.82	0.4	0.88	0.41	0.9	0.76	0.97	1.51	0.76	0.57
Al_2O_3	21.01	20.99	23.48	22.34	20.26	21.23	20.51	21.68	20.4	20.89	19.18	21.44	20.08	21.55	20.02	19.09	20.75	19.9
$Fe_2O_3^{Ta}$	2.43	2.37	1.99	3.07	3.7	2.34	2.76	2.68	3.15	2.74	3.21	2.67	3.45	3.13	3.64	5.45	3	2.67
MnO	0.3	0.21	0.17	0.34	0.18	0.25	0.39	0.24	0.19	0.37	0.2	0.32	0.19	0.2	0.19	0.27	0.19	0.25
MgO	0.14	0.53	0.15	0.18	0.75	0.15	0.05	0.27	0.55	0.2	0.58	0.12	0.65	0.52	0.74	1.58	0.48	0.27
CaO	0.83	0.98	0.42	0.82	2.3	1.04	0.69	1.19	1.98	0.84	1.97	0.37	1.99	2.21	2.48	3.5	1.83	1.28
Na_2O	9.75	4.25	6.37	5.57	5.9	9.49	10.65	7.58	6.92	8.52	6.23	6.19	6.38	7.29	5.94	5.83	7.52	7.1
K_2O	6.11	8.42	5.4	8.4	7.8	6.35	5.64	7.14	7.52	6.38	7.75	6.24	7.34	5.66	7.31	6.7	7.43	7.12
P_2O_5	0.02	0.19	0.04	0.02	0.32	0.04		0.07	0.22	0.03	0.17	0.04	0.27	0.16	0.32	0.74	0.18	0.05
LOI	3.89	2.17	1.59	0.62	2	4.22	3.23	0.71	1.06	0.74	0.83	1.35	2.25	0.72	2.33	1.18	0.93	1.23
Sum	100.76	100.17	100.41	100.42	100.49	100	99.81	100.7	100.08	100.67	99.67	100.53	100.19	100.71	100.33	100.58	100.59	99.65
Sc		2			2				2	2	2	2	2	1	2	5	2	2
Ni									20		20		20			40		
Cr													nd					
Co	6	15	8	9	17	9	8	11	16	9	9	9	6	13	11	11	9	7
V	9	24	11	23	41	14	6	18	28	11	25	10	33	34	38	82	27	13
Ba	4	194	5	88	536	7	2	66	277	4	201	6	401	218	455	898	232	18
Rb	229	167	190	363	128	222	296	177	154	274	142	282	125	101	123	112	154	168
Sr	14	673	15	235	1747	40	3	267	857	8	745	22	1274	1002	1492	1816	722	66
Y	39.1	42.6	37.1	43.2	30.2	29.3	39	39	41.1	64.9	43.4	80.9	32.2	31.3	32.8	34.2	37.4	43.2
Zr	1132	431	1142	1909	460	995	1915	837	456	1781	598	1837	436	467	424	292	433	751
Nb	262	162	238	371	130	224	321	216	155	387	180	428	137	142	129	109	143	213

Tabela 2: Continuação.

	Rochas Subvolcanicas												Rochas Plutonicas					
	138B	**139A**	**139B**	**140A**	**140B**	**141C**	**141D**	**142A**	**143A**	**144A**	**144B**	**144D**	**138A**	**139C**	**141A**	**141B**	**142B**	**143B**
La	240	227	273	261	165	194	203	227	211	225	180	274	179	238	180	195	180	217
Ce	363	457	386	342	310	288	244	391	418	411	357	471	344	423	350	390	363	405
Pr	31.8	54.1	34.9	30	35.4	23.6	16.3	39.8	48.6	39.9	41.9	49	39.3	45.3	40.5	45	42.7	42.3
Nd	77.5	173	80.8	69	112	50.4	29.3	109	144	97.3	129	123	122	133	129	146	121	110
Sm	8.62	22.9	8.27	8.04	14.7	5.7	3.13	13.2	18.6	13.5	18.1	16	16.1	15.2	17	19.5	15.9	13.9
Eu	1,030	5,110	0.956	1,440	3,910	0.82	0.421	2,170	4,120	0.902	4,490	1,040	3,600	4,780	4,170	4,680	3,190	1,780
Gd	5.42	13.1	5.06	5.11	8.66	3.64	2.4	8.17	10.8	8.83	11.6	11.3	9.41	8.93	9.47	11.5	9.73	8.25
Tb	0.99	1.92	0.89	0.87	1.24	0.62	0.57	1.23	1.64	1.59	1.62	2.04	1.38	1.26	1.4	1.59	1.46	1.32
Dy	6.45	10.1	5.68	5.78	6.69	4.06	4.14	7.33	8.79	10.6	8.9	13	7.17	6.83	7.73	8.23	7.85	7.84
Ho	1.47	1.76	1.28	1.44	1.19	0.95	1.11	1.39	1.63	2.41	1.74	2.87	1.31	1.25	1.31	1.4	1.49	1.61
Er	4.69	4.68	4.14	5.01	3.23	3.29	4.46	4.5	4.52	7.47	4.86	8.62	3.69	3.63	3.81	3.76	4.33	4.84
Tm	0.752	0.614	0.684	0.896	0.419	0.568	0.879	0.657	0.606	1,150	0.588	1,400	0.512	0.444	0.497	0.487	0.589	0.737
Yb	5.27	3.44	4.76	6.67	2.63	4.23	7.34	4.32	3.83	7.69	4.31	9.58	3.07	2.75	3.03	2.79	3.46	4.58
Lu	0.848	0.484	0.755	1,140	0.424	0.713	1,200	0.695	0.599	1,230	0.61	1,430	0.462	0.415	0.439	0.381	0.473	0.701
Hf	21.9	9.6	22	36	9.5	19	34.1	17.8	11.5	34.5	12.6	39.2	9.4	10.9	9	6.4	10	15.6
Pb	25	10	21	40	11	23	46	17	13	29	16	32	12	18	11	7	12	17
Th	37.6	15.4	35.4	62.9	16.4	38.1	56.8	27.7	17.1	51.4	19.5	56.8	15.7	16.9	14.8	9.97	15	25.6
U	8.32	4.42	6.35	7.13	3.21	8.25	15.8	6.07	3	11.1	4.25	5.35	2.87	2.61	2.71	1.73	2.77	4.81

[a]Todo ferro presente nas amostras foi analisado como ferro total na forma de ferro férrico

Tabela 3: Norma CIPW calculada no GeoChemical Data ToolKIT (GCDkit) para amostras de rochas da área de estudo (continua).

	Amostras de rochas subvolcanicas											
	138B	139A	139B	140A	140B	141C	141D	142A	143A	144A	144B	144D
Q	0.00	0.352	1623.00	0.00	0.00	0.00	0.00	0.00	0.00	0.00	0.00	0.043
C	0.00	3626.00	6544.00	2654.00	0.00	0.00	0.00	0.00	0.00	0.00	0.00	3957.00
Or	36452.00	50065.00	32025.00	49698.00	46335.00	38011.00	33677.00	42216.00	44595.00	37729.00	45980.00	36975.00
Ab	28737.00	36193.00	54105.00	29333.00	24196.00	24694.00	30396.00	30139.00	25719.00	36480.00	30004.00	52527.00
Na	0.00	3645.00	1829.00	3942.00	5905.00	0.00	0.00	4056.00	2474.00	0.00	1560.00	1579.00
Ne	25189.00	0.00	0.00	9673.00	14087.00	27505.00	24374.00	18438.00	17906.00	19246.00	12423.00	0.00
Ac	2223.00	0.00	0.00	0.00	0.00	2144.00	2519.00	0.00	0.00	0.122	0.00	0.00
Ns	1307.00	0.00	0.00	0.00	0.00	0.826	3008.00	0.00	0.00	0.00	0.00	0.00
Di	3531.00	0.00	0.00	0.00	2876.00	4343.00	3072.00	1194.00	4965.00	3450.00	5950.00	0.00
Hy	0.00	2433.00	1868.00	0.00	0.00	0.00	0.00	0.00	0.00	0.00	0.00	2608.00
Ol	1069.00	0.00	0.00	2420.00	1792.00	0.596	1680.00	1523.00	0.523	0.908	0.201	0.00
Mt	0.00	1080.00	0.903	1394.00	1692.00	0.00	0.00	1219.00	1427.00	1187.00	1456.00	1207.00
Il	0.572	1617.00	0.686	0.748	1909.00	0.604	0.316	1019.00	1572.00	0.759	1681.00	0.774
Ap	0.048	0.453	0.095	0.047	0.762	0.096	0.00	0.166	0.523	0.071	0.404	0.095
Sum	99128.00	99463.00	99678.00	99909.00	99553.00	98819.00	99041.00	99969.00	99703.00	99952.00	99660.00	99765.00

Tabela 3: Continuação

Amostras de rochas plutônicas					
138A	139C	141A	141B	142B	143B
0.00	0.00	0.00	0.00	0.00	0.00
0.00	0.00	0.00	0.00	0.00	0.00
43666.00	33467.00	43483.00	39708.00	43975.00	42285.00
28797.00	38760.00	28082.00	25372.00	24683.00	35543.00
4646.00	9380.00	6558.00	6212.00	0.953	1504.00
13854.00	12440.00	12206.00	13060.00	21156.00	13465.00
0.00	0.00	0.00	0.00	0.00	0.00
0.00	0.00	0.00	0.00	0.00	0.00
2932.00	0.457	3094.00	5206.00	5839.00	3895.00
0.00	0.00	0.00	0.00	0.00	0.00
1561.00	2216.00	1707.00	3109.00	0.033	0.44
1578.00	1422.00	1665.00	2473.00	1365.00	1210.00
1734.00	1445.00	1866.00	2889.00	1449.00	1094.00
0.643	0.379	0.763	1757.00	0.427	0.119
99412.00	99967.00	99425.00	99787.00	99880.00	99557.00